POLITEHNICA University of Bucharest
FACULTY OF MATERIALS SCIENCE AND ENGINEERING
Bucureşti, Splaiul Independenţei, nr. 313, Sector 6, cod poştal 060042
http://www.sim.pub.ro

PhD Thesis Summary

Specific Aspects Regarding the Behaviour of Some Titanium Based Alloys During Thermomechanical Processing

Author: Mohammed Hayder Ismail Alluaibi

Scientific coordinator: Prof. Habil. Dr. Eng. Vasile Dănuț COJOCARU

DOCTORAL COMMITTEE

President	Prof. Habil. Dr. Eng. Constantin Stelian STAN	From	POLITEHNICA University of Bucharest
Scientific supervisor	Prof. Habil. Dr. Eng. Vasile Dănuț COJOCARU	From	POLITEHNICA University of Bucharest
Scientific reviewer	Prof. Dr. Eng. Leandru-Gheorghe BUJOREANU	From	Gheorghe Asachi Technical University of Iasi
Scientific reviewer	Prof. Dr. Eng. Anna NOCIVIN	From	OVIDIUS University of Constanta
Scientific reviewer	Prof. Dr. Eng. Doina RADUCANU	From	POLITEHNICA University of Bucharest

Bucharest, 2021

POLITEHNICA University of Bucharest
FACULTY OF MATERIALS SCIENCE AND ENGINEERING
Bucureşti, Splaiul Independenţei, nr. 313, Sector 6, cod poştal 060042
http://www.sim.pub.ro

Table of Contents

Chapter 8: Results and discussion (Experimental program III)

Chapter 9: General conclusions, personal contributions, recommendations and future research directions

Abstract

In this thesis, different experimental programs have been developed focusing on designing appropriate thermomechanical processing routes to correlate the effects induced by thermomechanical processing to the microstructure and mechanical properties of Ti-6246 alloy in order to obtain an appropriate combination of strength and ductility properties. The developed experimental programs have a different level of complexity. The processing routes were based on the main parameter, which is the β-transus temperature of Ti-6246 alloy located close to 935°C. The developed mechanical processing experiments are at temperatures below, close to and above the β-transus temperature, while the developed thermal processing experiments are at temperatures below, close to and above the β-transus temperature. Experimental results revealed deformations of varying intensity in the initial grains and colonies of the alloy, while the deformed grains were fully recrystallised and the deformed α-Ti/β-Ti colonies were fully regenerated by different treatments such as treatment of annealing, solution and ageing. In order to obtain high-intensity deformation, the chosen deformation temperature must be above β-transus temperature, while to obtain high-strength and/or high-ductility properties, the chosen deformation temperature must be below β-transus temperature.

Keywords: Titanium alloy; Microstructure; Mechanical properties; Thermomechanical processing; Fracture surface; Optical microscopy; Scanning electron microscopy; X-ray diffraction.

Chapter 1: Introduction

1.3. Problem statement

Although many researchers aim to designate the correlation between microstructural characteristics and mechanical behaviour for titanium alloys, the exact correlation was not fully established. In fact, the challenges that often arise in order to establish this full correlation are not one single reason but several reasons or a combination of many parameters that influence each other concerning microstructure characteristics and mechanical behaviour. Additionally to these complexities, most of the microstructure characteristics directly affect each other as the prior β grain size affects the size of the resulting α colony, the grain boundaries width of α layer and other characteristics as well. Because of this intercorrelation of microstructure characteristics, it is almost impossible to change only one microstructure characteristic to study its influence on mechanical behaviour. Moreover, to obtain functional dependencies of the microstructure characteristics that have an explicit effect on mechanical behaviour, it is necessary to describe the microstructure's characteristics accurately and quantitatively in order to achieve a complete data matrix about these characteristics.

Many advanced methods of hot deformation process like forging, rolling, others, along with different heat treatments like annealing, solution, ageing, others, are generally applicable to titanium alloys. In this regard, some of these thermomechanical processes will contribute to the present work of the thesis by manipulating in the microstructure features of Ti-6246 alloy in an attempt to improve their mechanical properties, and it is possible to use microstructure characteristics as important input variables through the data that will obtain during many experiments that will conduct to contribute to the creation of insights about the microtexture of Ti-6246 alloy, and the establishment of functional dependencies for mechanical behaviour depending on the microstructure characteristics.

The microstructure characteristics of Ti-6246 alloy will be studied on a micrometre scale using optical microscopy and scanning electron microscopy. Mechanical tests will also perform in order to accurately characterise the various microstructure features and their close association with each other. Thereby, the mechanical behaviour of various compositions can be predicted and applied to novel alloys with desired mechanical behaviour. Functional dependencies between microstructure characteristics and mechanical behaviour can be designated, and it is possible to use these functional dependencies to develop physical-based models.

1.4. Thesis structure

The structure of the thesis is organised into two parts. The first part includes the theoretical part, which is organised into four chapters. **Chapter 1** consists of the general background, literature review, problem statement and thesis structure. **Chapter 2** deals with the fundamental aspects of titanium and its alloys. **Chapter 3** deals with different technical aspects that can be employed for titanium and its alloys. **Chapter 4** presents a detailed review of typical thermomechanical processing routes for titanium and its alloys.

The second part includes the experimental part, which is organised into five chapters. **Chapter 5** presents a detailed description of the research questions/hypotheses, research objectives, research strategy and methodology used to conduct the experimental programs that include the alloy sampling system and equipment used in this study. **Chapter 6** presents the results and

discussion regarding the first experimental program with their conclusions for hot plastic deformation by upsetting Ti-6246 alloy with a dead-weight dropping machine followed by an annealing treatment. **Chapter 7** and **Chapter 8** present the results and discussion of the second and third experimental programs with their conclusions regarding hot plastic deformation by rolling-mill and treatments of solution and ageing of Ti-6246 alloy. **Chapter 9** provides general conclusions, personal contributions, recommendations and future research directions related to the present thesis. References and results dissemination are included at the end of the thesis.

Chapter 2: Metallurgical aspects of titanium and its alloys with their applications

2.1. Physico-chemical constitution of titanium and its alloys

The alloying elements for titanium alloys are classified as follows (Walter et al., 1988; Ezugwu and Wang, 1997; Pederson, 2004; Pardhi, 2010; Guuo, 2012):

1) Stabilisers of α-type: they consist of elements that dissolve in the α-Ti phase, and the most common ones added to titanium to strengthen it are oxygen and aluminium.
2) Stabilisers of β-type: they consist of elements that dissolve in the β-Ti phase. These stabilisation elements can divide into β-isomorphous like Mo and V and β-eutectoid like Mn and Cr. Table 2.1 shows examples of different elements of α, β and neutral stabilisers, along with their position in the lattice crystal (interstitial or substitutional).
3) Neutral stabilisers: consist of Si, Sn and Zr elements and have a negligible/modest influence on β-transus temperature due to their large solubility in α-Ti and β-Ti phases. These elements can strengthen the α-Ti phase or sometimes the β-Ti phase.

Table 2.1

The position of alloying element in the crystal lattice (Lütjering and Williams, 2007; Cherukuri, 2008; Veiga et al., 2012)

Type of crystal lattice	**α-Stabilizer**				**β-Stabilizer**							**Neutral**	
					β-isomorphous		**β-eutectoid**						
	Al	O	N	C	Mo	V	Fe	Cr	Mn	H	Ni	Sn	Zr
Substitutional	√				√	√						√	√
Interstitial		√	√	√			√	√	√	√	√		

2.2. Classification of titanium alloys

Titanium alloys can be classified into five groups:

1) Titanium alloys of α-type include only α-stabilisers that affect the α-Ti phase in the microstructure or can combine with neutral alloying elements (Weiss and Semiatin, 1999; Peters et al., 2003; Cherukuri, 2008; Veiga et al., 2012).
2) Titanium alloys of near-α type include α-stabilisers and small quantities of β-stabilisers that decrease the β-transus temperature (Ezugwu and Wang, 1997; Weiss and Semiatin, 1999; Peters et. al., 2003).
3) Titanium alloys of (α + β) type consist of a dual-phase microstructure with high quantities of α-Ti and β-Ti stabilisers at ambient temperature (Semiatin et al., 1997; Welsch et al., 1994; Peters et al. 2003; Liu, 2005; Mullen et al., 2007; Veiga et al., 2012).

4) Titanium alloys of near-β type include β-stabilisers and small quantities of α-stabilisers that increase the β-transus temperature (Welsch et al., 1994; Weiss and Semiatin, 1998; Liu, 2005).
5) Titanium alloys of β-type include very large quantities of β-stabilisers that stabilise the β-Ti phase at ambient temperature (Pardhi, 2010; Ahmed et al., 2012).

2.4. Solid-state transformations and nature of titanium alloys phases

The nature of the phases of titanium alloys of (α + β) type can divide into equilibrium and non-equilibrium phases. The main equilibrium phases such as: α-Ti, α_2-Ti and β-Ti phases. Some of the important non-equilibrium phases such as: α'-Ti and α''-Ti phases (Donachie, 2000; Liu, 2005; Guuo, 2012).

2.5. Crystallization kinetics and microstructure evolution of titanium and its alloys

Like many other metals (e.g. Ca, Fe, Co, Zr, Sn, Ce and Hf), titanium can form different crystal structures. However, each crystal structure is stable at a certain temperature range (Leyens and Peters, 2003). Pure (unalloyed) titanium can categorise into two main allotropic forms. The first form represents the low temperature (up to 882±2°C), known as a Hexagonal Closed-Packed (HCP) crystal structure. This form refers to the α-Ti phase. The second form represents the high temperature (above 882°C), and a HCP structure transformed into a Body-Centred Cubic (BCC) crystal structure, which refers to the β-Ti phase (Partridge, 1967; Flower, 1990; Askeland et al., 2010; Richardson, 2016). The Ti-6246 alloy contains somewhat more β-stabilisers than the Ti-64 alloy and thus has more equilibrium of β-Ti phase at ambient temperature. There is some confusion in the scientific literature concerning Ti-6246 alloy because this alloy is sometimes called a titanium alloy of (α + β) type (Boyer et al., 1994; Bein and Béchet, 1996; Jackson et al., 2001) or a titanium alloy of near-β type (Walter et al., 1988; Donachie, 2000; Roder et al., 2003). In fact, it belongs to the group of titanium alloys of (α + β) type depending on the alloy's chemical components.

Chapter 3: Advanced methods of phenomena characterisation occurring during thermomechanical processing of titanium-based alloys

3.1. A brief introduction

This chapter mainly deals with bulk deformation processes (see Fig. 3.1), which include mechanical processing, in addition to some heat treatments such as treatment of annealing, solution and ageing, which will apply in the present research study, where these tools will combine to study the effect of thermomechanical processing applied on Ti-6246 alloy that will use in the present research study to achieve a suitable combination of microstructure and mechanical properties.

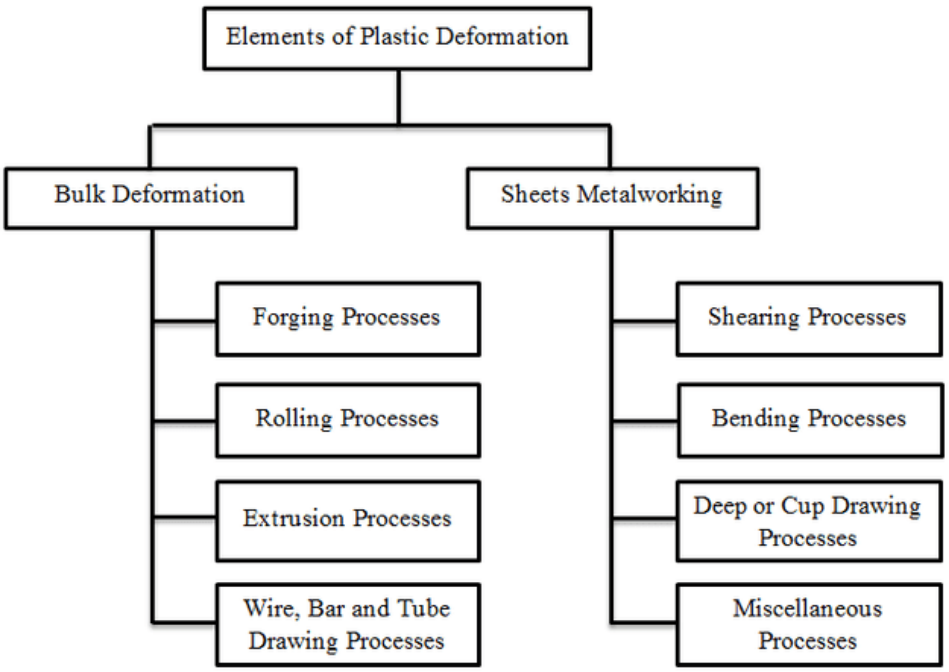

Fig. 3.1 *Classification of plastic deformation elements (Groover, 2007; Irthiea, 2013).*

Chapter 4: Thermomechanical processing routes of titanium-based alloys

4.1. A brief introduction

There are several thermomechanical processing performed on titanium-based alloys. The β-transus temperature is a central point in the topic of thermomechanical processing as it serves to determine the α-Ti and β-Ti phase transformations (Joshi, 2006). The response of titanium alloys (α, near-α, (α + β), near-β/metastable-β and β alloys) to thermomechanical processing depends on the alloy chemical composition, which plays an important role in the evolution of mechanical properties within the alloy microstructure, and the type of thermomechanical processing applied responsible for changes within the microstructure of the alloy in terms of microtexture morphologies, grains size and phase transformations evolution, as well as influencing grain boundaries in the alloy structure. Thermomechanical processing defined as a metallurgical process that combines mechanical processing/plastic deformation by forging, rolling, compression, etc., and thermal processing/heat treatments such as annealing, solution, ageing, etc. in similar or different variables of temperature, duration and cooling rate in a single processing route. Through these three variables, it is possible to induce large evolution in microstructural/mechanical properties.

Chapter 5: Research objectives and methodology

5.1. Research questions and hypotheses

The present thesis is focused on the following main research questions:

- What are the microstructure characteristics in the manufactured Ti-6246 alloy when applying additional thermomechanical processing?
- What are phasic transformations occurring in Ti-6246 alloy during thermomechanical processing?

- What are the functional dependencies between microstructure – exhibited mechanical properties of Ti-6246 alloy induced by thermomechanical processing?

5.2. Research objectives

The main objectives of this thesis can be summarised as follows:

1. To increase knowledge and obtain a further understanding of the Ti-6246 alloy in terms of microstructure evolution during thermomechanical processing and the influence of microstructure on exhibited mechanical properties.
2. To study the influence of mechanical processing (by hot-deformation performed below, close to and above β-transus temperature) on strength and ductility properties evolution in Ti-6246 alloy.
3. To study the influence of thermal processing (by solution treatments performed below, close to and above β-transus temperature, and by ageing treatments) on strength and ductility properties evolution in Ti-6246 alloy.
4. To optimise mechanical properties of Ti-6246 alloy by coupling deformation processing (hot-deformation) with thermal treatments (solution and ageing treatments) in order to obtain a suitable combination of strength and ductility properties.
5. To achieve the thesis objectives, different investigative tools have been combined. These tools are optical microscopy (OM), scanning electron microscopy (SEM), energy-dispersive X-ray spectroscopy (EDS/EDXS), X-ray diffraction (XRD) and different mechanical testing such as tensile strength and microhardness testing.

5.3. Research strategy

The research strategy was focused on designing appropriate thermomechanical processing routes to correlate the effects induced by the thermomechanical processing on microstructure and exhibited mechanical properties, aiming to obtain an appropriate/suitable combination of strength and ductility properties. The main parameter that was taken into consideration when designing the applied thermomechanical processing routes is the β-transus temperature of Ti-6246 alloy (located close to 935°C), where the developed mechanical processing experiments are at temperatures below, close to and above the β-transus temperature, as well as the developed thermal processing experiments at temperatures below, close to and above the β-transus temperature.

The first experimental program (see Fig. 5.1) consists of mechanical processing (by hot-deformations - **HD**) of as-received (**AR**) Ti-6246 alloy in a wide temperature range, from well below to well above the β-transus temperature, such as: 800°C (**HD1**), 900°C (**HD2**), 1000°C (**HD3**) and 1100°C (**HD4**). In all cases, the hot-deformation was performed by dead-weight dropping testing, assuring the same potential deformation energy. Considering that the thermal processing can drastically influence the alloy's microstructure, in order to have a basis for comparison, it has been chosen to apply the same thermal treatment after mechanical processing, i.e. the annealing treatment (**AT1 - AT4**) was performed at 950°C (slightly above β-transus temperature ~ 935°C). The treatment duration was fixed to 30mins before slow cooling of the heat-treated samples (furnace cooling). All obtained structural states were investigated from a microstructural and mechanical point of view in order to determine the

correlation among applied thermomechanical processing parameters, obtained microstructural features and exhibited mechanical properties.

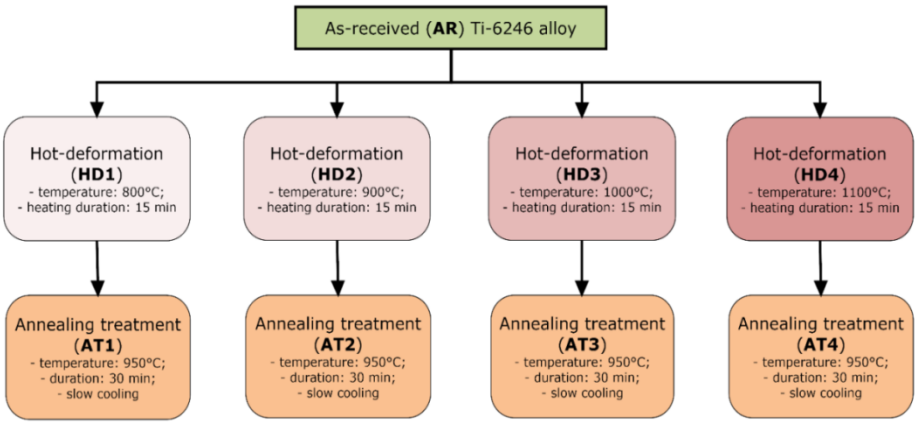

Fig. 5.1 *Schematic representation of the first experimental program of thermomechanical processing applied to Ti-6246 alloy.*

Based on the results obtained from the first experimental program, it has been chosen to continue the thermomechanical processing of Ti-6246 alloy, aiming to investigate in depth the correlation between thermomechanical processing applied close to β-transus temperature, the obtained microstructural features and the exhibited mechanical properties. It has been chosen to investigate the mechanical processing at the following temperature: 900°C (close below the β-transus temperature ~ 935°C) and 1000°C (above the β-transus temperature ~ 935°C) in order to apply solution treatments (**ST**) at the following temperatures: 800°C (well below the β-transus temperature ~ 935°C), 900°C (close below the β-transus temperature ~ 935°C) and 1000°C (above the β-transus temperature ~ 935°C), followed by final ageing treatment (**A**) at 600°C.

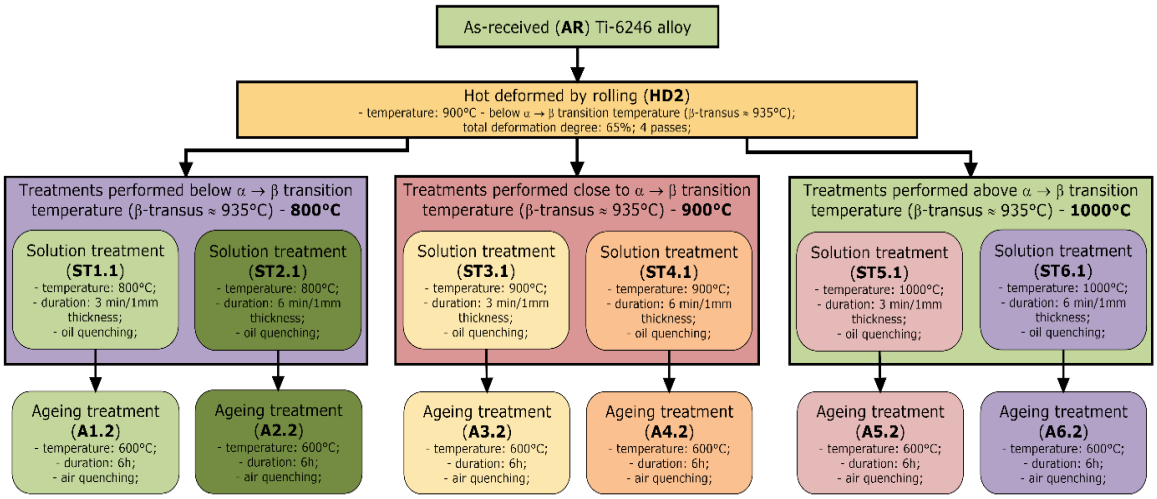

Fig. 5.2 *Schematic representation of the second experimental program of thermomechanical processing applied to Ti-6246 alloy.*

The second experimental program (see Fig. 5.2) consists of mechanical processing, by hot-rolling, at 900°C (**HD2**) of as-received (**AR**) Ti-6246 alloy. After hot-rolling, the first set of HD2 processed samples were solution treated (**ST**) at 800°C, with different treatment durations: 3min/mm of sample thickness (**ST1.1**), and 6min/mm of sample thickness (**ST2.1**). The thermal processing continued with a final ageing treatment (**A**) performed at 600°C, with treatment duration of 6h, resulting in the following states: **A1.2** (ST1.1 + A) and **A2.2** (ST2.1

+ A). The second set of HD2 processed samples were solution treated (**ST**) at 900°C, with different treatment durations: 3min/mm of sample thickness (**ST3.1**), and 6min/mm of sample thickness (**ST4.1**). The thermal processing continued with a final ageing treatment (**A**) performed at 600°C, with treatment duration of 6h, resulting in the following states: **A3.2** (ST3.1 + A) and **A4.2** (ST4.1 + A). Finally, the third set of HD2 processed samples were solution treated (**ST**) at 1000°C, with different treatment durations: 3min/mm of sample thickness (**ST5.1**), and 6min/mm of sample thickness (**ST6.1**). The thermal processing continued with a final ageing treatment (**A**) performed at 600°C, with treatment duration of 6h, resulting in the following states: **A5.2** (ST5.1 + A) and **A6.2** (ST6.1 + A). All obtained structural states were investigated from a microstructural and mechanical point of view in order to determine the correlation between applied thermomechanical processing parameters, obtained microstructural features and exhibited mechanical properties.

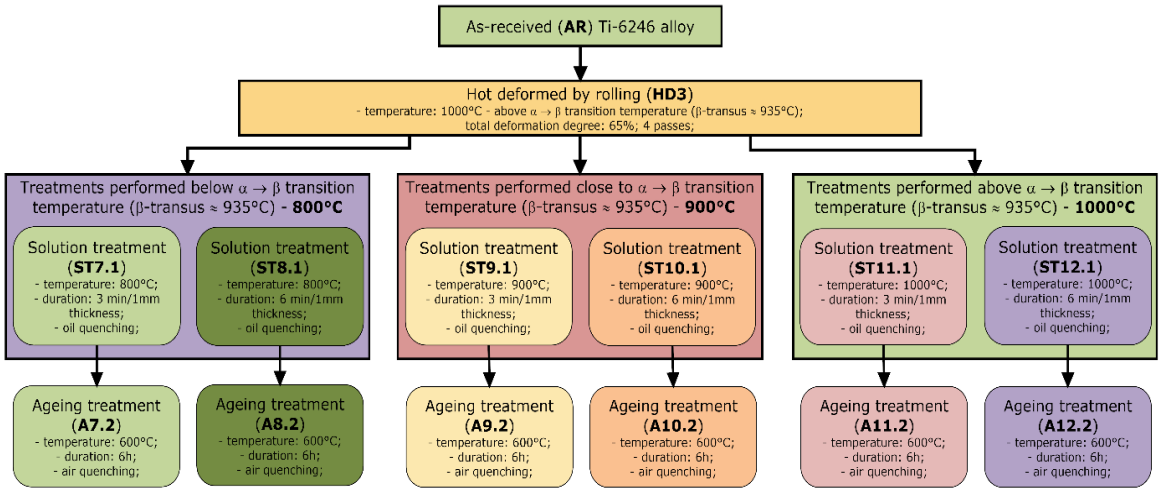

Fig. 5.3 *Schematic representation of the third experimental program of thermomechanical processing applied to Ti-6246 alloy.*

The third experimental program (see Fig. 5.3) consists of mechanical processing, by hot-rolling, at 1000°C (**HD3**) of as-received (**AR**) Ti-6246 alloy. After mechanical processing at 1000°C (HD3), a similar thermal processing route was applied, as in the second experimental program, in order to compare the obtained data. The first set of HD3 processed samples were solution treated (**ST**) at 800°C, with different treatment durations: 3min/mm of sample thickness (**ST7.1**), and 6min/mm of sample thickness (**ST8.1**). The thermal processing continued with the final ageing treatment (**A**) performed at 600°C, with treatment duration of 6h, resulting in the following states: **A7.2** (ST7.1 + A) and **A8.2** (ST8.1 + A). The second set of HD3 processed samples were solution treated (**ST**) at 900°C, with different treatment durations: 3min/mm of sample thickness (**ST9.1**), and 6min/mm of sample thickness (**ST10.1**). The thermal processing continued with the final ageing treatment (**A**) performed at 600°C, with treatment duration of 6h, resulting in the following states: **A9.2** (ST9.1 + A) and **A10.2** (ST10.1 + A). Finally, the third set of HD3 processed samples were solution treated (**ST**) at 1000°C, with different treatment durations: 3min/mm of sample thickness (**ST11.1**), and 6min/mm of sample thickness (**ST12.1**). The thermal processing continued with the final ageing treatment (**A**) performed at 600°C, with treatment duration of 6h, resulting in the following states: **A11.2** (ST11.1 + A) and **A12.2** (ST12.1 + A). All obtained structural states were investigated from a microstructural and mechanical point of view in order to determine the correlation between

applied thermomechanical processing parameters, obtained microstructural features and exhibited mechanical properties.

5.4. Research methodology

The commercial titanium alloy possessing chemical composition Ti-6(wt.%)Al-2(wt.%)Sn-4(wt.%)Zr-6(wt.%)Mo (Ti-6246) was obtained from ***S.C. ZIROM TITANIUM S.A.***, (Giurgiu, Romania). Then the samples were taken and processed from the parent alloy according to a studied system to investigate how the thermomechanical processing affects the microstructural and exhibited mechanical properties of Ti-6246 alloy. Samples were prepared for analytical-descriptive investigations using various devices and equipment such as: Scanning Electron Microscopy (SEM) - TESCAN VEGA II – XMU (TESCAN, Brno, Czech Republic); Optical Microscopy (OM) - OLYMPUS, Model - BX 51M; Malvern Panalytical Empyrean (Malvern Panalytical BV, Almelo, Netherlands) diffractometer for microstructural investigation. Also, INSTRON 3382 (INSTRON, Norwood, MA, USA); INNOVATEST Falcon 500 equipment (INNOVATEST Europe BV, Maastricht, Netherlands) for mechanical investigation.

Chapter 6: Results and discussion (Experimental program I)

6.1. Microstructure evolution during thermomechanical processing

6.1.1. Microstructure analysis of as-received (AR) Ti-6246 alloy

Fig. 6.1 shows optical microscopy (OM) images of as-received (AR) Ti-6246 alloy. One can observe that the microstructure consists of a large number of millimetre-sized grains, with an average grain size exceeding 2mm, besides millimetre-sized grains, the microstructure shows the presence of a small fraction of sub-millimetre-sized grains, with an average grain size close to 500μm (see Fig. 6.1.a). All grains show the presence of multiple colonies, possessing different spatial orientations, formed of alternate fine lamellae/plate-like structures of two different phases, typical for Widmanstätten/basket-weave type morphology (see Fig. 6.1.b). Fig. 6.1 also shows typical SEM-BSE (SEM - backscattered electrons) microstructural images of as-received (AR) Ti-6246 alloy at different magnifications. One can observe that the grain consists of adjacent colonies of alternate lamellae/plate-like structures with the same orientation (see Fig. 6.1.c). One can identify the presence of two constituent phases, the first one - coloured in light-grey (indicating the presence of alloying elements with a higher atomic number) and, the second one - coloured in dark-grey (indicating the presence of alloying elements with a lower atomic number) (see Fig. 6.1.d). Both phases show an average lamella/platelet thickness below 1μm (see Fig. 6.1.d). The XRD analysis shows that the observed phases are identified as α-Ti and β-Ti phases, respectively (see Fig. 6.1.e). The α-Ti phase showed a hexagonal close-packed (HCP) crystalline structure and with the lattice parameters close to a = 0.294nm and c = 0.467nm, while the β-Ti phase showed a body-centred cubic (BCC) crystalline structure and with lattice parameters close to a = 0.327nm.

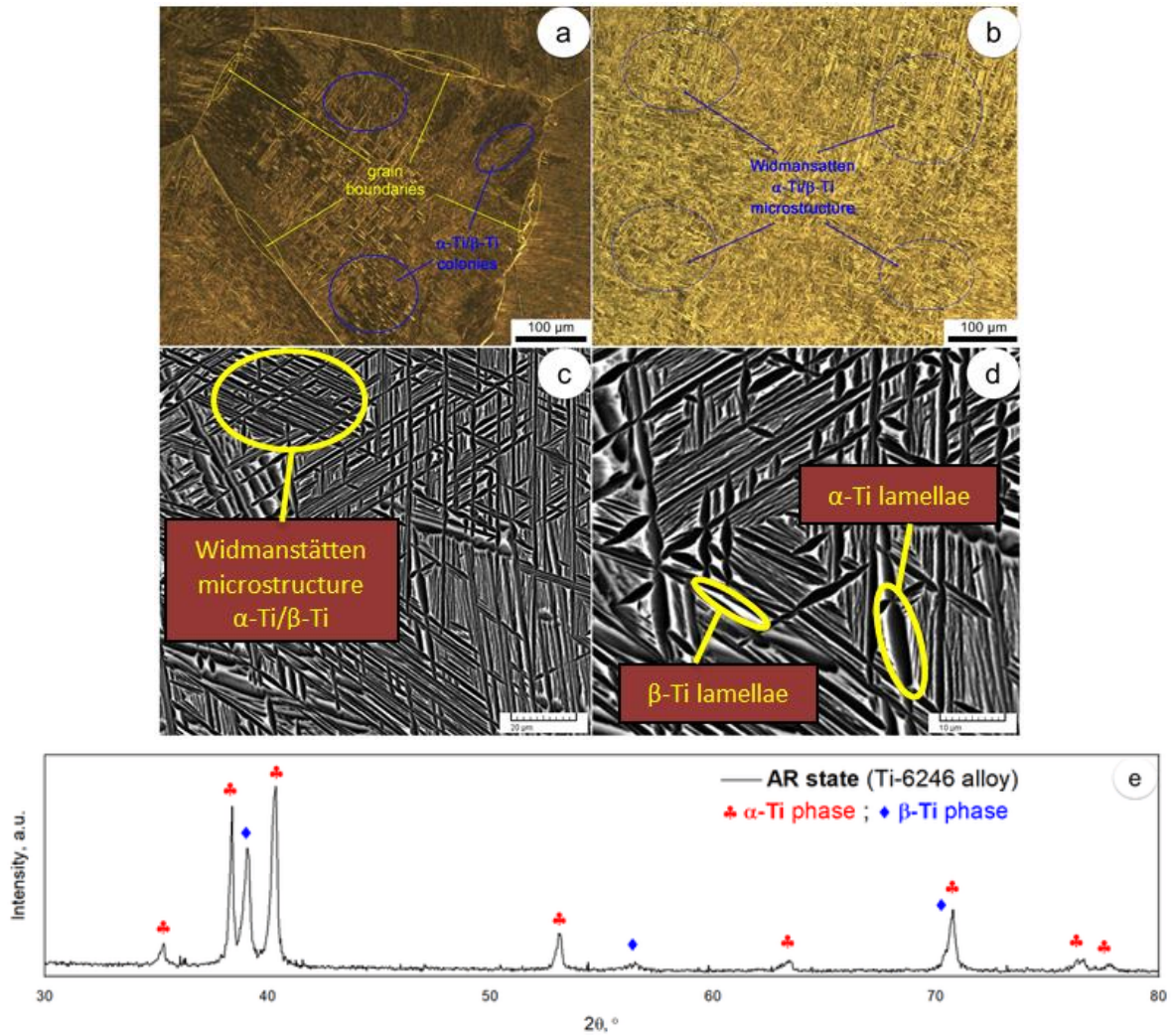

Fig. 6.1 *Images of as-received (AR) case; OM images in different investigation areas (a and b); SEM images in different magnifications (c and d); XRD spectra image (e).*

The dispersion maps of the main alloying elements (Ti, Al, Sn, Zr, Mo and Fe) within the microstructure are presenting in Fig. 6.3.b to Fig. 6.3.g. The EDS analysis of the dispersion maps also indicates the presence of two main constituent phases, the first one enriched in α-stabilising elements, such as: Ti (Fig. 6.3.b) and Al (Fig. 6.3.c), and depleted in β-stabilising elements, such as: Mo (Fig. 6.3.d) and Zr (Fig. 6.3.e), the second one enriched in β-stabilising elements, such as: Mo (Fig. 6.3.d) and Zr (Fig. 6.3.e), and depleted in α-stabilising elements, such as: Ti (Fig. 6.3.b) and Al (Fig. 6.3.c). All other alloying elements show an almost uniform distribution within the microstructure (Sn- Fig. 6.3.f and Fe - Fig. 6.3.g). Based on EDS analysis, one can assume that the α-Ti phase enriched in Ti and Al, therefore coloured in dark-grey, while the β-Ti phase enriched in Mo and Zr, therefore coloured in light-grey. Fig. 6.3.h shows the EDS spectra of Ti-6246 alloy in the AR case. The computed chemical composition is presenting in Table 6.1. Overall, the microstructure analysis shows that the Ti-6246 alloy obtained by double VAR synthesis route consists of a homogenous microstructure with millimetre-sized grains, each grain showing multiple coherent colonies presence of alternate α-Ti/β-Ti lamellae/plate-like structures. No segregations or other defects such as porosities, inclusions, etc., were detected.

Table 6.1

Chemical composition of as-received (AR) Ti-6246 alloy

Element	%, wt.	%, at	Abs. error [%]	Rel. error [%]
Titanium	81.54	82.55	2.44	2.76
Aluminium	6.33	11.36	0.33	4.77
Tin	1.85	0.75	0.05	2.94
Zirconium	3.91	2.08	0.16	3.79
Molybdenum	6.24	3.15	0.24	3.54
Iron	0.14	0.12	0.12	2.77

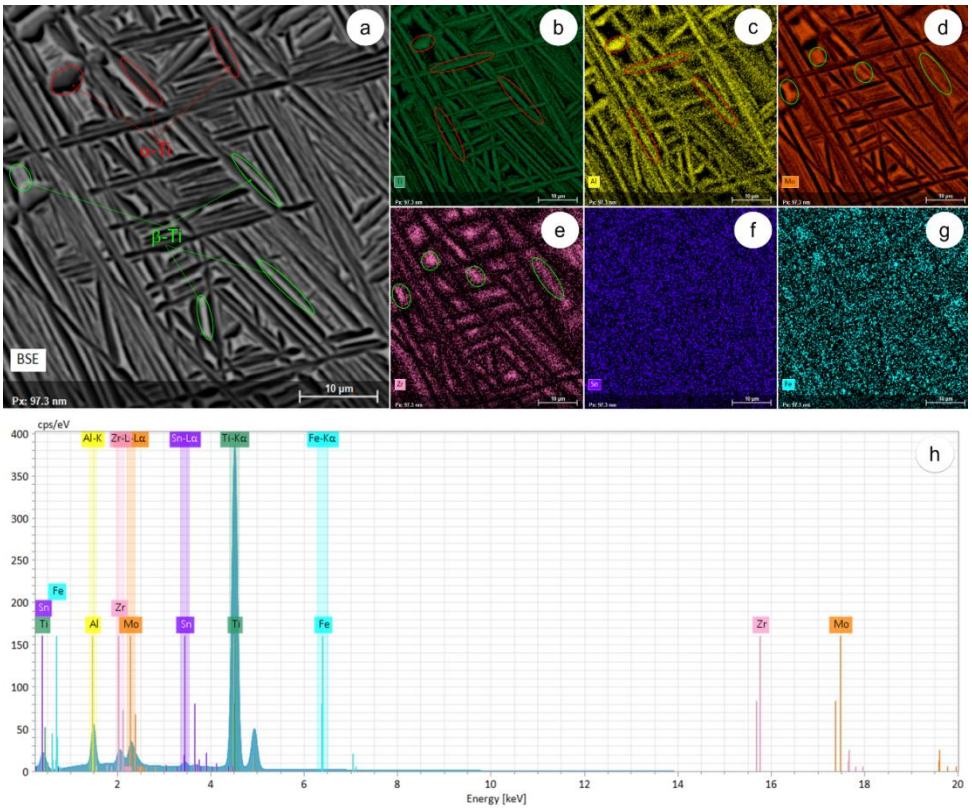

Fig. 6.2 *Distribution maps of main alloying elements in as-received (AR) Ti-6246 alloy: SEM-BSE microstructural image (a); SEM-EDS distribution map of Ti (b); Al (c); Mo (d); Zr (e); Sn (f); Fe (g); global EDS spectra (h).*

6.1.2. Microstructure analysis of hot deformation (HD) cases

Fig. 6.3 shows typical images of the microstructure of Ti-6246 alloy by OM for the hot-deformed (HD) cases at different temperatures. Considering the hot deformation (HD1) case (see Fig. 6.3.a), performed at 800°C well below the β-transus temperature of Ti-6246 alloy (≈ 935°C), for 15 mins, with a total deformation degree of 57%, one can observe a low deformation of the initial α-Ti/β-Ti colonies texture along the forging direction (FD) that shows preferred spatial orientation that differs from the AR Ti-6246 alloy due to the low deformation temperature, indicating a low deformation of the initial grains that show an elongated morphology aligned with the FD. Also, no secondary phases generated from the initial α-Ti and β-Ti phases observed. When analysing the hot deformation (HD2) case (see Fig. 6.3.b), performed at 900°C below close to the β-transus temperature of Ti-6246 alloy (≈ 935°C), for 15 mins, with a total deformation degree of 60%, one can observe higher deformation of the

initial α-Ti/β-Ti colonies texture along FD compared to the case of hot deformation (HD1), where the deformed colonies show a preferred spatial orientation that differs from the AR Ti-6246 alloy due to the close deformation temperature from the β-transus temperature, inferring that the initial grains deformed to a higher degree than the deformed initial grains in the hot deformation (HD1) case and also show an elongated morphology aligned with the FD. No secondary phases observed in this case. By examining the hot deformation (HD3) case (see Fig. 6.3.c), performed at 1000°C above the β-transus temperature of Ti-6246 alloy (≈ 935°C), for 15 mins, with a total deformation degree of 62%, one can observe the occurrence of recrystallisation of deformed initial grains and heavy deformation of the initial α-Ti/β-Ti colonies along FD compared to the AR Ti-6246 alloy due to higher deformation temperature compared to the cases of the hot deformation (HD1 and HD2). No secondary phases observed in the hot deformation (HD3) case. By seeing the hot deformation (HD4) case (see Fig. 6.3.d), performed at 1100°C well above the β-transus temperature of Ti-6246 alloy (≈ 935°C), for 15 mins, with a total deformation degree of 64%, one can observe the heavy deformation of the initial α-Ti/β-Ti colonies within the deformed initial grain and along the FD compared the AR Ti-6246 alloy due to higher deformation temperature compared to the cases of hot deformation (HD1, HD2 and HD3), as also observed secondary α''-Ti phase belonging to the orthorhombic crystalline system with thick lamellar/acicular-like structures dispersed within the β-Ti phase matrix.

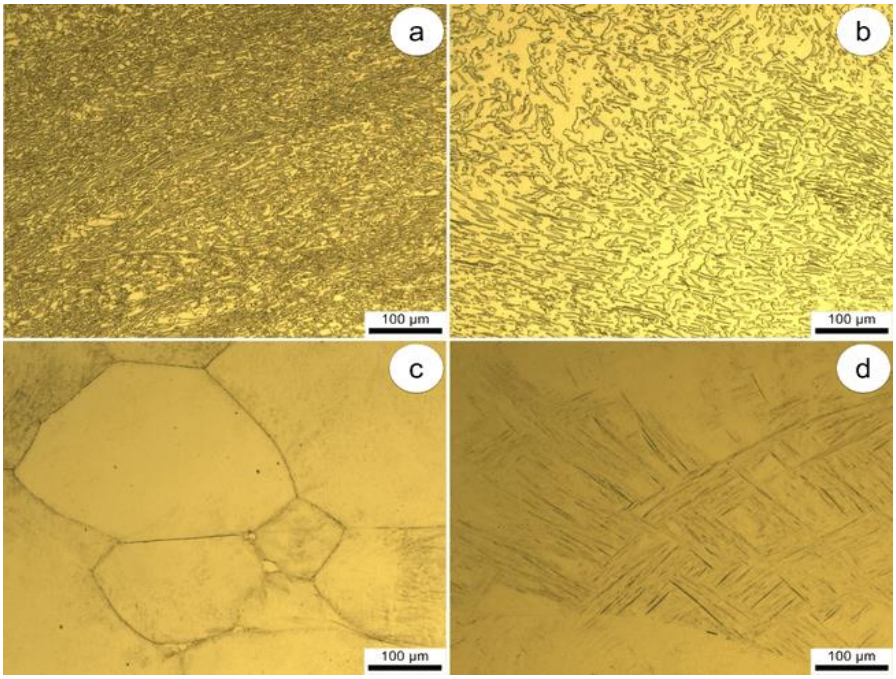

Fig. 6.3 *OM images of hot deformation (HD1) case at 800°C (a); hot deformation (HD2) case at 900°C (b); hot deformation (HD3) case at 1000°C (c); hot deformation (HD4) case at 1100°C (d).*

Fig. 6.4 shows typical images of the microstructure of Ti-6246 alloy by SEM-BSE for the hot-deformed (HD) cases at different temperatures. In the case of hot deformation (HD1), one can observe the presence of coarse lamellar/plates-like structures of the initial α-Ti and β-Ti phases along FD that show a preferred spatial orientation different from the AR Ti-6246 alloy, besides the coarse random/irregular morphologies of both initial phases, as observed, the secondary fine lamellar structures of the initial α-Ti phase dispersed within the initial β-Ti phase (see Fig.

6.4.a), based on these observations, it can say that the initial grains have a low deformation showing an elongated morphology with the FD and the grains boundaries separating the deformed colonies are thick. No secondary phases observed in the hot deformation (HD1) case. In the case of hot deformation (HD2), one can observe the lamellar/plates-like structures of the initial α-Ti phase dispersed in the initial β-Ti phase matrix along FD with relatively thinner thickness with different spatial orientations compared to the AR Ti-6246 alloy, as observed, the absence of secondary fine lamellar structures of the initial α-Ti phase dispersed within the initial β-Ti phase when compared with the hot deformation (HD1) case (Fig. 6.4.b), according to these observations, it can affirm that the initial grains have a higher deformation magnitude with an elongated morphology aligned with FD and grain boundaries separating the deformed colonies are thinner compared to the hot deformation (HD1) case. No thermally induced secondary phases observed in this case.

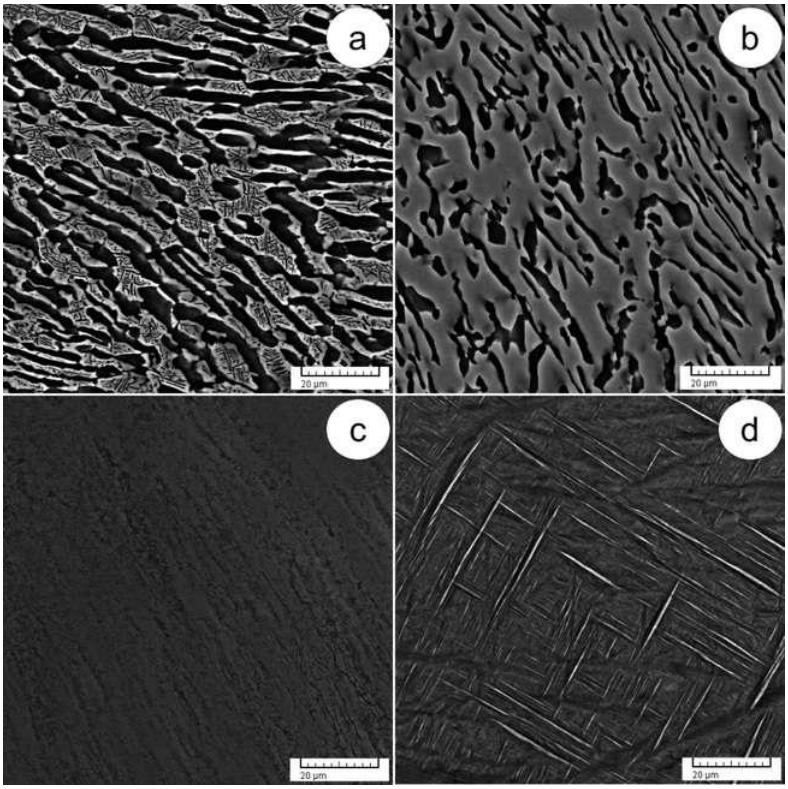

Fig. 6.4 *SEM-BSE images of hot deformation (HD1) case at 800°C (a); hot deformation (HD2) case at 900°C (b); hot deformation (HD3) case at 1000°C (c); hot deformation (HD4) case at 1100°C (d).*

In the case of hot deformation (HD3), it can be observing the heavily deformed of initial grains and the dense deformation of adjacent α-Ti/β-Ti colonies within the grains compared to the AR Ti-6246 alloy and the hot deformation (HD1 and HD2) cases that performed below the β-transus temperature, where these colonies separate by thin boundaries due to the high deformation temperature (1000°C) and the applied heavy deformation, and these colonies have spatial orientations that differ from the initial orientations of α-Ti/β-Ti colonies (see Fig. 6.4.c). Secondary phases are not present within the microstructure. In the case of hot deformation (HD4), it can be observing the deformations for α-Ti/β-Ti colonies within grains and these colonies separate by thin boundaries compared to the AR Ti-6246 alloy and similarly aligned to the hot deformation (HD3) case due to the high deformation temperature (1100°C) and application of the heavy deformation. Deformed colonies have spatial orientations that not

similar to the AR Ti-6246 alloy (see Fig. 6.4.d). The presence of thermally induced secondary α''-Ti phase also observed within the microstructure. The secondary α''-Ti phase belongs to the orthorhombic crystalline system with coarse lamellar/acicular-like structures in parallel orientations and showing a preferred spatial orientation with the initial β-Ti phase depending on the special Burgers relation between β-Ti/α''-Ti phases.

6.1.3. Microstructure analysis of annealing treatment (AT) cases

Fig. 6.5 shows typical images of the microstructure of Ti-6246 alloy by OM for the annealing treatment (AT) cases at the same temperatures. In the case of AT1 treatment (see Fig. 6.5.a), performed at 950°C above close to the β-transus temperature of Ti-6246 alloy (≈ 935°C), for 30 mins, after the HD1 case, performed at 800°C well below the β-transus temperature, it can observe that the deformed grains completely recrystallised along with the deformed α-Ti/β-Ti colonies texture that completely regenerated as alternate thin lamellae/plate-like structures compared to the HD1 case. These deformed colonies separated by grains boundaries have different spatial orientations within the grains. The secondary phases induced from the initial phases not observed due to the applied slow cooling in the case of AT1 treatment. In the case of AT2 treatment (see Fig. 6.5.b), performed at 950°C above close to the β-transus temperature of Ti-6246 alloy (≈ 935°C), for 30 mins, after the HD2 case, performed at 900°C a bit below the β-transus temperature, it is possible to observe the complete recrystallisation of the deformed grains and the complete regeneration in the texture of the deformed α-Ti/β-Ti colonies as alternate thin lamellar-like structures separated by grains boundaries with the morphology of Widmanstätten/basket-weave type in different spatial orientations within the grains compared to the HD2 case. An increase in the grain size and a decrease in the thickness of the lamellar structures can observe in comparison with the case of AT1 treatment, and no secondary phases observed in the microstructure due to the applied AT conditions. In the case of AT3 treatment (see Fig. 6.5.c), performed at 950°C above close to the β-transus temperature of Ti-6246 alloy (≈ 935°C), for 30 mins, after the HD3 case, performed at 1000°C above the β-transus temperature, one can observe the complete recrystallised in the deformed grains besides the complete regeneration of the deformed α-Ti/β-Ti colonies in the HD3 case with alternate thin lamellar/acicular-like structures separated by grains boundaries that show preferred spatial orientations. Continuous increase in grains size and decrease in thickness of lamellar/acicular-like structures can observe compared to the case of AT2 treatment and the formation of Widmanstätten/basket-weave morphology. Also, no secondary phases are observed within the microstructure due to the appropriate duration of AT and the applied slow cooling rate that tends to form large grains. In the case of AT4 treatment (see Fig. 6.5.d), performed at 950°C above close to the β-transus temperature of Ti-6246 alloy (≈ 935°C), for 30 mins, after the HD4 case, performed at 1100°C well above the β-transus temperature, it is possible to observe the occurrence complete recrystallisation of deformed grains along with the deformed α-Ti/β-Ti colonies that completely regenerated in the HD4 case that form alternate thin lamellar/acicular-like structures separated by grains boundaries that show preferred spatial orientations and the microstructure includes the morphology of the Widmanstätten/basket-weave. The grains still showed an increase in size compared to the aforementioned AT cases with a fine dispersion of lamellar/acicular-like structures. The secondary α''-Ti phase returned to the initial β-Ti phase due to sufficient conditions to AT.

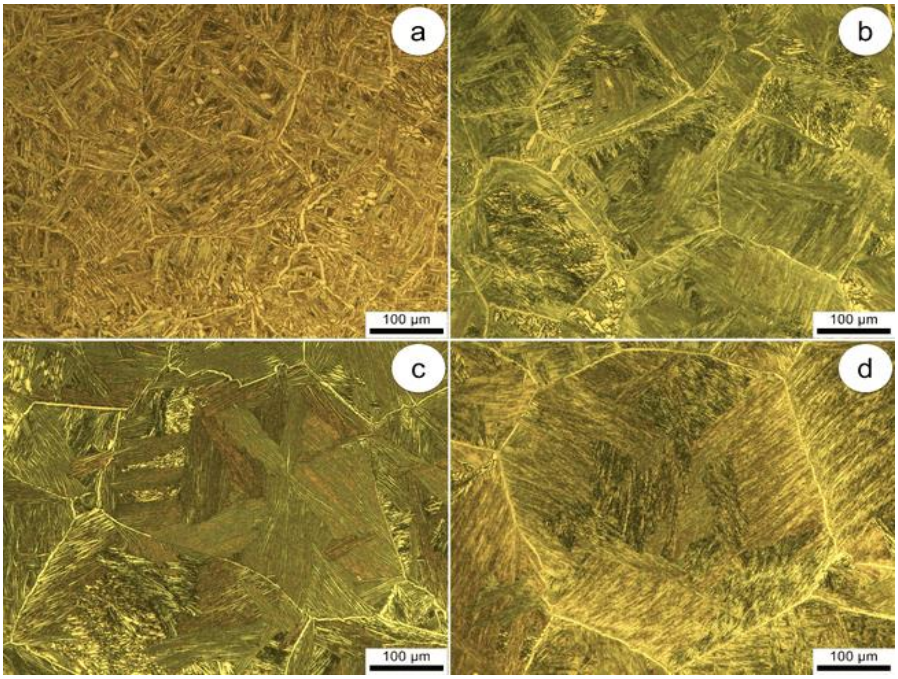

Fig. 6.5 *OM images of annealing treatment (AT1) case at 950°C (a); annealing treatment (AT2) case at 950°C (b); annealing treatment (AT3) case at 950°C (c); annealing treatment (AT4) case at 950°C (d).*

Fig. 6.6 shows typical images of the microstructure of Ti-6246 alloy by SEM-BSE for the annealing treatment (AT) cases at the same applied temperature. Observations of the case of AT1 treatment (see Fig 6.6.a) are the complete recrystallisation of the deformed grains and refinement of deformed α-Ti/β-Ti colonies that separated by the grain boundaries that form alternate thin lamellae/plate-like structures compared to HD1 case. The α-Ti/β-Ti colonies show preferred spatial orientations within the grains. The fine dispersion of lamellar structure within the β-Ti phase matrix is still present as in the HD1 case in addition to optimising the texture of deformed α-Ti/β-Ti colonies and the appearance of Widmanstätten/basket-weave morphology, and the secondary phases did not find in this case during the application of AT conditions. Considering the case of AT2 treatment (see Fig. 6.6.b), one can observe the completely recrystallised grains can observe in the HD2 case and the deformed α-Ti/β-Ti colonies that completely refinement as alternate thin lamellar-like structures separated by grains boundaries with preferred spatial orientations inside the grains, also, the increase in the grain size can observe when compared with the case of AT1 treatment due to the slow cooling rate. As observed, the optimisation of the texture of deformed α-Ti/β-Ti colonies and the presence of Widmanstätten/basket-weave morphology within the microstructure compared to the HD2 case. This case did not experience the presence of thermally induced secondary phases from the initial α-Ti and β-Ti phases as a result of applied AT conditions. By examining the case of AT3 treatment (see Fig. 6.6.c), it is possible to observe that the deformed grains completely recrystallised and the deformed α-Ti/β-Ti colonies completely regenerated when compared with the HD3 case, and this case contains thin lamellar/acicular-like structures separated by grains boundaries that show preferred spatial orientations, and the grains still increased in size compared to the case of AT2 treatment. Besides the presence of Widmanstätten/basket-weave morphology, it can observe a significant optimisation in the deformed α-Ti/β-Ti colonies texture and an increase in their thickness compared to the HD3

case. Within the microstructure of this case, no secondary phases observed due to the applied conditions of AT. When analysing the case of AT4 treatment (see Fig. 6.6.d), one can observe the complete recrystallised of the deformed grains and the complete regeneration of the deformed α-Ti/β-Ti colonies compared with the HD4 case and formation of alternate thin lamellar/acicular-like structures separated by grains boundaries with preferred spatial orientations, besides the continuous increase in the size of the grains compared to the AT cases that mentioned before. Also, the large grain junction area can be seeing. Optimisation in deformed α-Ti/β-Ti colonies and increased their thickness compared with the HD4 case can see, in addition to the presence of Widmanstätten/basket-weave morphology and the return of secondary α''-Ti phase generated in the HD4 case to the initial β-Ti phase due to the applied AT conditions.

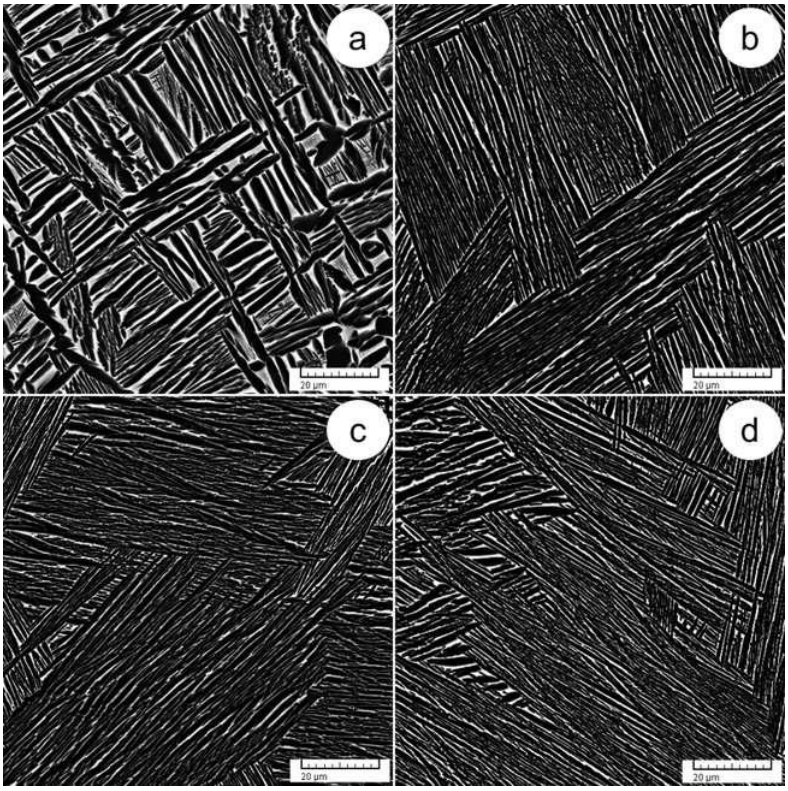

Fig. 6.6 *SEM-BSE images of annealing treatment (AT1) case at 950°C (a); annealing treatment (AT2) case at 950°C (b); annealing treatment (AT3) case at 950°C (c); annealing treatment (AT4) case at 950°C (d).*

6.2. Mechanical properties evolution during thermomechanical processing

By engineering strain-stress curves obtained from tensile testing for all thermomechanically processed cases, the following mechanical properties were determined: ultimate tensile strength (σ_{UTS}), 0.2% yield strength ($\sigma_{0.2\%}$), elongation to fracture (ε_f) during tensile testing in addition to microhardness (HV1). Table 6.2 shows the values of mechanical properties taken into consideration.

The strength properties of HD1 case increased slightly while the ductility decreased significantly compared to the AR Ti-6246 alloy, as a result of the fine lamellar precipitations of the α-Ti phase within the β-Ti phase along with the appearance of defects in the microstructure, confirming OM and SEM-BSE microstructural observations (Fig. 6.3.a and 6.4.a). The strength properties of the HD2 case decreased, and the ductility increased compared to the HD1 case, due to the higher deformation magnitude within the microstructure, resulting

in the absence of fine lamellar precipitations of the α-Ti phase within the β-Ti phase, and the decrease in the volumetric fraction of the α-Ti phase, and the increase in the volumetric fraction of the β-Ti phase, confirming OM and SEM-BSE microstructural observations (Fig. 6.3.b and 6.4.b). The microhardness of the HD3 case presented a very slight increase compared to the HD2 case due to the mechanism of work hardening, as the defects within the microstructure increased, causing an increase in the hardness of the material. In the tensile test, the strength properties slightly decreased while the ductility increased slightly compared to the HD2 case due to the thermomechanical processing performed in the β-Ti phase field, decreasing the volumetric fraction of the α-Ti phase and increase the volumetric fraction of the β-Ti phase, supporting OM and SEM-BSE microstructural observations (Fig. 6.3.c and 6.4.c). The HD4 case performed in the β-Ti phase-field showed a continuous increase in the volumetric fraction of the β-Ti phase and a decrease in the volumetric fraction of the α-Ti phase in addition to the generation of strengthening particles of the secondary α''-Ti phase dispersed within the β-Ti phase matrix, based on these observations, the HD4 case exhibited a slight increase in the microhardness and ductility and a slight decrease in the strength properties, supporting OM and SEM-BSE microstructural observations (Fig. 6.3.d and 6.4.d).

Table 6.2

Recorded mechanical properties for processed Ti-6246 alloy in the first experimental program

Structural state	**Mechanical properties**			
	Microhardness, HV1	Ultimate tensile strength, σ_{UTS} [MPa]	0.2 yield strength, $\sigma_{0.2\%}$ [MPa]	Elongation to fracture, ε_f [%]
As-received (**AR**)	305.2±16.9	1057±14	967±11	12.9±1.8
Hot-deformed at 800°C (**HD1**)	331.4±7.1	1101±12	972±11	3.5±0.8
Hot-deformed at 900°C (**HD2**)	291.6±4.6	1015±11	908±12	5.1±0.5
Hot-deformed at 1000°C (**HD3**)	292.1±9.2	1007±12	901±10	5.5±0.4
Hot-deformed at 1100°C (**HD4**)	295.4±5.1	1001±11	901±12	5.8±0.5
HD1 + Annealing treated: T = 950°C; t = 30min; FQ[(a)] (**AT1**)	323.1±14.2	1184±13	1051±13	8.3±1.1
HD2 + Annealing treated: T = 950°C; t = 30min; FQ[(a)] (**AT2**)	333.7±20.2	1191±12	1057±15	8.2±0.9
HD3 + Annealing treated: T = 950°C; t = 30min; FQ[(a)] (**AT3**)	341.3±18.5	1208±13	1063±13	7.5±1.1
HD4 + Annealing treated: T = 950°C; t = 30min; FQ[(a)] (**AT4**)	356.5±25.1	1221±11	1072±12	6.2±0.8
(a) Furnace quenching (FQ).				

In the cases of annealing treatment (AT), the mechanical properties showed important evolutions depending on the analysis of the microstructure (see Fig. 6.5 and 6.6), and if the treatment conditions are sufficient, will lead to the recrystallisation in the deformed grains, as well as regeneration of the deformed α-Ti/β-Ti colonies, decreasing the defects of the deformed microstructure and increases the properties of strength and ductility compared to the hot-deformed (HD) cases. Also, the slow cooling rate prevented the generation of secondary phases within the microstructure. The microhardness of the AT1 treatment case slightly decreased compared to the HD1 case due to the stress-relieving. The strength and ductility properties of tensile testing increased as a result of recrystallisation and regeneration of the alloy microstructure during the applied conditions of AT, in line with OM and SEM-BSE microstructural observations (Fig. 6.5.a and 6.6.a). The strength and ductility properties

increased in the AT2 treatment case compared to the HD2 and the AT1 treatment case due to the application of AT above the alloy transition temperature for the deformed microstructure close to the alloy transition temperature, leading to modification of the deformations occurring within the microstructure, no large increase in strength properties showed compared to the AT1 treatment case due to the large grain size, where from the mechanical viewpoint, mechanical properties favour smaller grains if higher strength properties desired, supporting OM and SEM-BSE microstructural observations (Fig. 6.5.b and 6.6.b). The strength and ductility properties increased in the AT3 treatment case compared to the HD3 case due to the effect of the applied AT conditions, modifying the deformed microstructure of Ti-6246 alloy, showing an improvement in mechanical properties. Besides, the AT3 treatment case showed less ductility compared to the AT1 and AT2 treatment cases due to the coarse lamellar structures of the α-Ti phase, increasing the strength of the material and decrease the ductility property, confirming OM and SEM-BSE microstructural observations (Fig. 6.5.c and 6.6.c). The microhardness increased in the AT4 treatment case compared to the HD4 case and the AT3 treatment case due to the effect of the applied AT conditions. The strength and ductility properties increased in the case of AT4 treatment compared to the HD4 case while the ductility decreased in this case compared to the aforementioned annealing treatment cases due to the coarser lamellar structures of the α-Ti phase within the β-Ti phase matrix, besides the degradation of the secondary α''-Ti phase and back to the initial β-Ti phase, causing this behaviour, confirming OM and SEM-BSE microstructural observations (Fig. 6.5.d and 6.6.d).

6.3. Conclusions

A thermomechanical processing route applied in the present study in order to investigate the evolutions occurring in the microstructure and mechanical properties of Ti-6246 alloy. The summarised conclusions are presented as following:

- During hot deformations cases, performed at different temperatures ranging from 800°C to 1100°C, deformations of varying severity occurred to the initial grains, in addition to deformations in the texture of the α-Ti and β-Ti constituent phases of Ti-6246 alloy, where in the hot deformation cases performed below the β-transus temperature at 800°C and 900°C, the deformations were low compared to the deformations performed above the β-transus temperature at 1000°C and 1100°C, therefore it is possible to progress with the hot deformation performed at temperatures not too far from the alloy's transition temperature (β-transus temperature ≈ 935°C) in subsequent experimental programs in order to investigate the effects of hot deformation on the final mechanical properties of the material. These deformations increase defects within the alloy microstructure. Consequently, the strength and ductility properties decreased. No secondary phases precipitated in the hot deformation cases, except for the one performed at 1100°C, where the secondary α''-Ti phase generated from the initial β-Ti phase.
- During annealing treatment cases, performed at a fixed temperature of 950°C, with treatment duration of 30 mins and slow cooling, the deformed grains and the texture of deformed α-Ti/β-Ti colonies modified, decreasing defects within the microstructure of Ti-6246 alloy compared to the hot deformation cases. Consequently, strength and ductility properties increased. No secondary phases precipitated in the annealing treatment cases.

Chapter 7: Results and discussion (Experimental program II)

7.1. Microstructure evolution during thermomechanical processing

7.1.1. Microstructure analysis of hot deformation (HD2) case

Fig. 7.1 shows the typical SEM-BSE microstructural images at different magnifications and XRD spectra image of hot-deformed (HD2) Ti-6246 alloy. One can observe the low deformation of the initial grains showing elongated morphology along the RD (see Fig. 7.1.a), because of the deformation temperature (900°C) performed below close to the β-transus temperature of Ti-6246 alloy, which is 935°C, and the high applied deformation (total deformation degree ≈ 59%). Although the grain boundaries are not shown in Fig. 7.1, but one can say that they tend to align along the RD, and the deformed α-Ti/β-Ti colonies separated by thick boundaries. Coarse initial α-Ti/β-Ti colonies show different spatial orientations from initial colonies in the AR case, and it is possible to see the high deformation of the texture of adjacent secondary α-Ti/β-Ti colonies with an average thickness close to 15µm (see Fig. 7.1.b). The XRD spectra of the HD2 case (see Fig. 7.1.c) shows that the diffraction peaks of both α-Ti and β-Ti phases are characterised by large widths (peak broadening), indicating a low grain-size for both α-Ti and β-Ti phases.

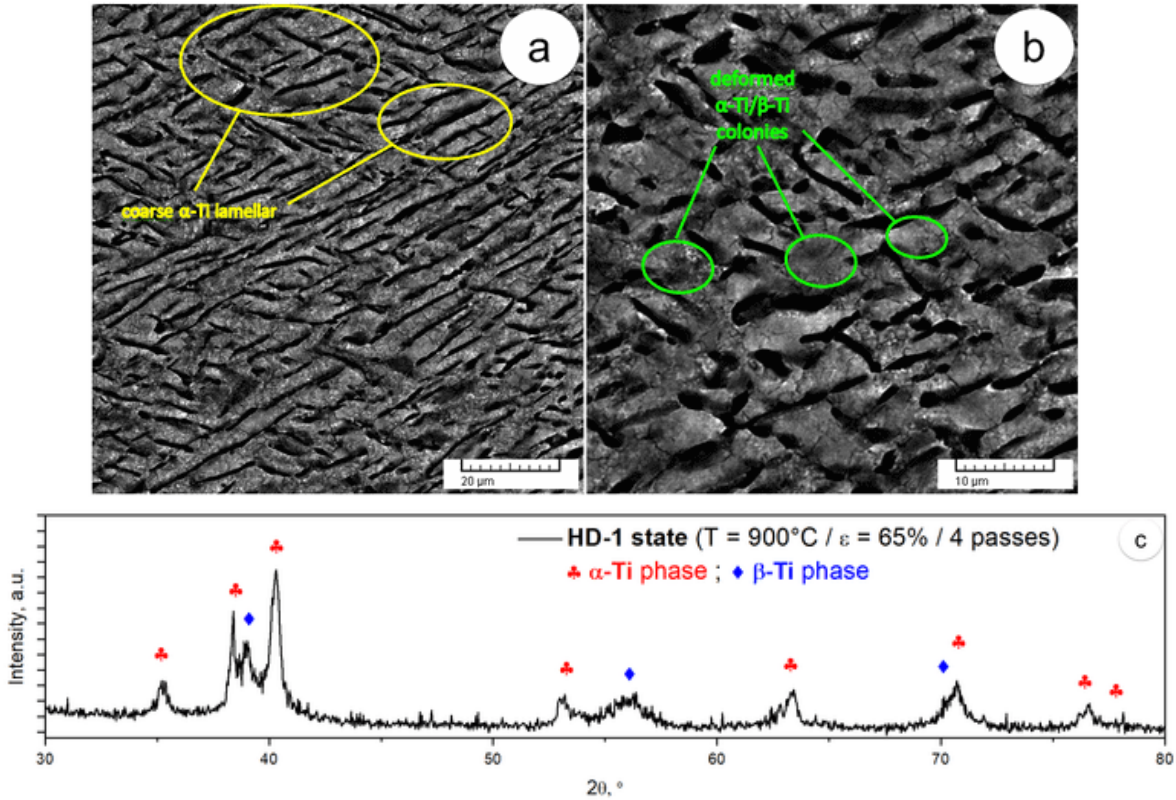

Fig. 7.1 *SEM-BSE images of hot-deformed (HD2) case in different magnifications (a and b); XRD spectra of HD2 case (c).*

7.1.2. Microstructure analysis of solution treatment (ST) cases

Fig. 7.2 shows typical SEM-BSE microstructural images of solution treated (ST) Ti-6246 alloy at different temperatures and durations. In the case of ST 1.1 treatment (see Fig. 7.2.a), performed well below the β-transus temperature (≈ 935°C), it is possible to observe that the deformed grains have fully recrystallised. Besides the presence of boundaries traces of the prior deformed colonies, both α-Ti and β-Ti phases were fully regenerated as alternate thin

lamellae/plate-like structures showing preferred spatial orientation in addition to the random/irregular coarse morphologies of the initial α-Ti phase. This case also revealed a fine-texture acicular structure presence identified as an α'-Ti phase, and this phase generated along with the initial α-Ti and β-Ti phases as a result of rapid cooling at ambient temperature. The secondary α'-Ti phase possesses the HCP crystalline system as with the crystalline system of the initial α-Ti phase and shows a preferred spatial orientation with the initial α-Ti phase based on the special Burgers relation between the α-Ti/α'-Ti phases. In the case of ST 3.1 treatment (see Fig. 7.2.b), performed below close to the β-transus temperature (≈ 935°C), one can observe that the deformed grains significantly recrystallised, resulting in the formation of random/irregular coarse morphologies of the initial α-Ti phase besides the thin lamellae/plate-like structural traces of initial α-Ti and β-Ti phases. The average thickness of α-Ti/β-Ti lamellae shows a higher thickness compared to the ST 1.1 treatment case. It can observe that the secondary α'-Ti phase, with a platelet-like morphology, finely dispersed, in the initial α-Ti phase, as a consequence of rapid cooling at ambient temperature. Observations of the ST 5.1 treatment case (see Fig. 7.2.c), performed above the β-transus temperature (≈ 935 ° C), are that the microstructure possesses a basket-weave type morphology and rapid cooling at 1000°C to ambient temperature produces a microstructure containing a structural mixture of lamellar/acicular fine dispersion and parallel platelets of large-sized. These parallel platelets represent a secondary α''-Ti phase which formed as a result of rapid cooling to the ambient temperature of the β-Ti phase. The α''-Ti phase possesses an orthorhombic crystalline system showing a preferred spatial orientation with the initial β-Ti phase based on the special Burgers relation between β-Ti/α''-Ti phases. It is worth mentioning that the initial α-Ti phase with random/irregular coarse morphologies fully melted in this case due to solution treatment (ST 5.1 case) performed in the β-Ti phase-field.

In the case of ST 2.1 treatment (see Fig. 7.2.d), performed well below the β-transus temperature (≈ 935°C), one can notice that the deformed grains have fully recrystallised. Both α-Ti and β-Ti phases were fully regenerated as alternate thin lamellae/plate-like structures showing preferred spatial orientation and random/irregular coarse morphologies of the initial α-Ti phase in addition to the presence of boundaries traces of the prior deformed colonies. The secondary α'-Ti phase possessing the HCP crystalline system as with the initial α-Ti phase crystalline system was formed due to the rapid cooling to the ambient temperature with the initial α-Ti and β-Ti phases, and contains fine dispersion of acicular structure within the α-Ti phase, showing the preferred spatial orientation with α-Ti phase based on the special Burgers relation between α-Ti/α'-Ti phases. In the ST 4.1 treatment case (see Fig. 7.2.e), performed below close to the β-transus temperature (≈ 935°C), it is possible to see that the deformed grains significantly recrystallised, and the microstructure containment of random/irregular coarse morphologies of the initial α-Ti phase and thin lamellae/plate-like structural traces of the initial α-Ti and β-Ti phases. This case presents the average thickness of α-Ti/β-Ti lamellae higher than the thickness of α-Ti/β-Ti lamellae in the ST 2.1 treatment case. One can observe the generation of secondary α'-Ti phase, with fine dispersion of platelet-like morphology in the initial α-Ti phase, due to rapid cooling at ambient temperature. By analysing the case of ST 6.1 treatment (see Fig. 7.2.f), performed above the β-transus temperature (≈ 935°C), one can observe that the microstructure possesses a basket-weave type morphology. During rapid cooling at a temperature of 1000°C to ambient temperature, the microstructure consists of a

structural mixture of a lamellar/acicular fine dispersion and large-sized parallel platelets formed within the microstructure. These parallel platelets belonging to the secondary α'-Ti phase formed due to rapid cooling in the β-Ti phase-field, and the α'-Ti phase possesses the orthorhombic crystalline system and shows a preferred spatial orientation with the initial β-Ti phase according to special Burgers relation between β-Ti/α''-Ti phases. Consideration should give to the full absence of initial α-Ti phase containing random/irregular coarse morphologies in this case due to heating above β-transus (≈ 935°C).

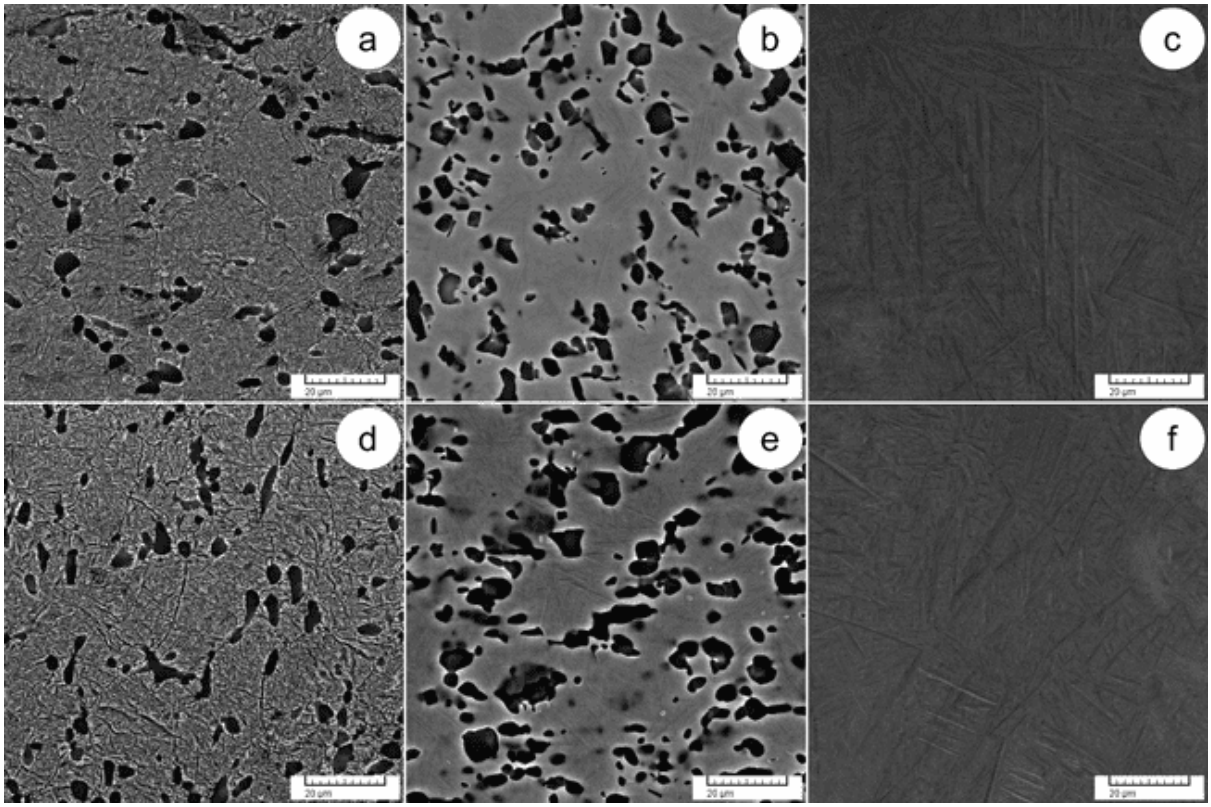

Fig. 7.2 *SEM-BSE images of solution treatment at 800°C (ST 1.1) case (a); solution treatment at 900°C (ST 3.1) case (b); solution treatment at 1000°C (ST 5.1) case (c); solution treatment at 800°C (ST 2.1) case (d); solution treatment at 900°C (ST 4.1) case (e); solution treatment at 1000°C (ST 6.1) case (f).*

Fig. 7.3 shows typical XRD spectra of solution treated (ST) states at different temperatures. In the case of ST 1.1 treatment, performed well below the β-transus temperature (≈ 935°C), one can observe diffraction peaks belonging to β-Ti, α-Ti and α'-Ti phases (see Fig. 7.3.a). The β-Ti phase classifies in the BCC crystalline system, with lattice parameters close to a = 0.327nm. The α-Ti and α'-Ti phases classify in the HCP crystalline system, and both show close lattice parameters (close to a = 0.294nm and c = 0.467nm), and thus difficult to distinguish between them. The differences in lattice parameters are due to supersaturation in β-stabilizers elements in the α''-Ti phase compared to the α-Ti phase. In the case of ST 3.1 treatment, performed below close to the alloy transition temperature (≈ 935°C), one can see diffraction peaks belonging to β-Ti, α-Ti and α'-Ti phases (see Fig. 7.3.b). Analysing the relative intensities of diffraction peaks, one can see the tendency of the phase texture along certain crystallographic directions, suggesting the preferred growth of crystallographic grains at all phases, supporting SEM-BSE microstructural observations (see Fig. 7.2.b). In the ST 5.1 treatment case, performed above the β-transus temperature (≈ 935°C), one can observe diffraction peaks

belonging to the α-Ti, β-Ti, α''-Ti phases and possibly α'-Ti phase (see Fig. 7.3.c). Due to the heating at 1000°C, i.e. in the β-Ti phase-field, during rapid cooling to ambient temperature, α''-Ti phase generated. The α''-Ti phase classifies in the orthorhombic crystalline system, with lattice parameters close to a = 0.296nm, b = 0.496nm and c = 0.468nm. Due to the close lattice parameters of both α-Ti and α'-Ti phases, only the α-Ti phase was considered. Analysing the relative intensities of diffraction peaks, one can notice texture directions showing the preferred growth of all phases within crystallographic grains, supporting SEM-BSE microstructural observations (see Fig. 7.2.c). In all cases, if one analyses the width of the diffraction peaks (peaks broadening) can see that the peaks indicate low-sized grains for all observed phases, supporting SEM-BSE microstructural observations (see Fig. 7.2.a - c).

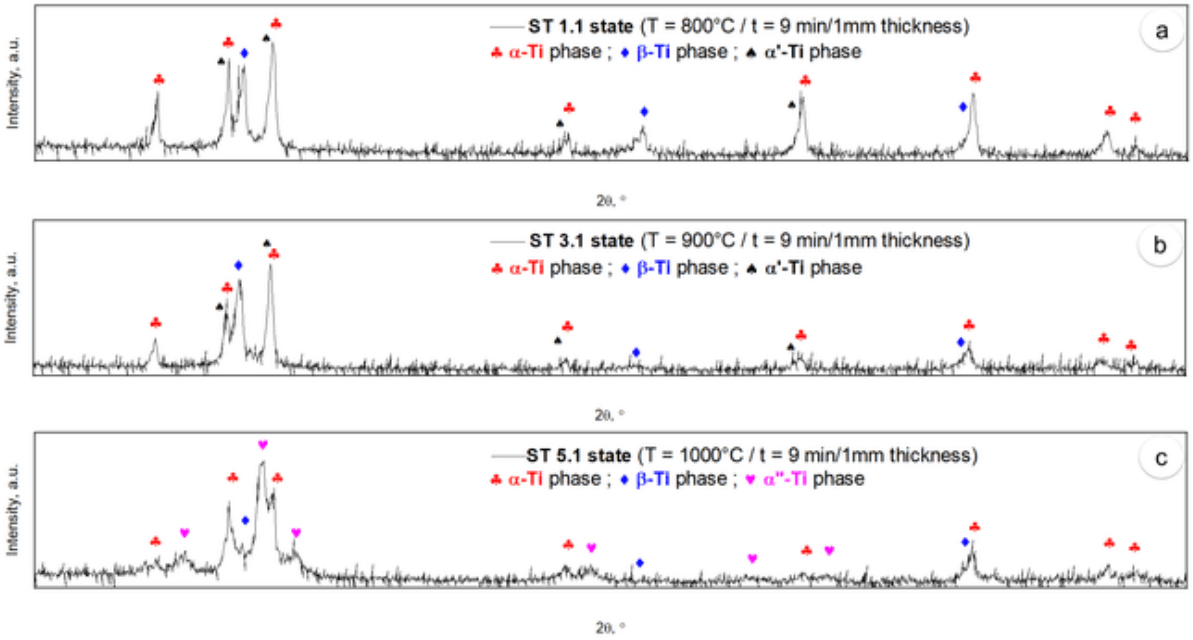

Fig. 7.3 *XRD spectra of solution treatment at 800°C (ST 1.1) case (a); solution treatment at 900°C (ST 3.1) case (b); solution treatment at 1000°C (ST 5.1) case (c).*

7.1.3. Microstructure analysis of ageing (A) cases

Fig. 7.4 shows typical SEM-BSE microstructural images of ageing treated (A) Ti-6246 alloy at fixed temperature and duration after solution treatment (ST). The microstructure of the ST 1.1 + A 1.2 treatment case (see Fig. 7.4.a) shows the same morphological concept compared to the ST 1.1 treatment case consisting of the textural dispersion of the initial α-Ti and β-Ti phases described before as the random/irregular coarse morphologies of the initial α-Ti phase and the alternate thin lamellae/plate-like structures of the initial α-Ti and β-Ti phases showing a preferred spatial orientation, as can also observe boundaries traces of colonies. In the application of the ageing treatment, the secondary α'-Ti phase with a fine acicular texture was not observed, indicating that the ageing treatment performed at 600°C with a treatment duration of 6h is sufficient to induce the transformation of the secondary α'-Ti phase to the initial α-Ti phase. The case of ST 3.1 + A 3.2 treatment (see Fig. 7.4.b) presents the same morphological aspect compared to the ST 3.1 treatment case in terms of random/irregular coarse morphologies of the initial α-Ti phase dispersed within the β-Ti phase matrix, but on the other hand, it is possible to observe that the lamellae/plate-like structures of the initial α-Ti and β-Ti phases are of delicate-size within the microstructure when compared with the ST 3.1 case. The secondary

α'-Ti phase transforms into the initial α-Ti phase during the application of ageing treatment. Analysing the ST 5.1 + A 5.2 treatment case (see Fig. 7.4.c), one can notice that the microstructure shows the morphology of the basket-weave type and involves alternate thin lamellar/plate-like structures of α-Ti and β-Ti phases. No secondary α'-Ti/α''-Ti phases were noticed in the microstructure of this case, as ageing treatment transformed the secondary α'-Ti/α''-Ti phases into the initial α-Ti/β-Ti phases.

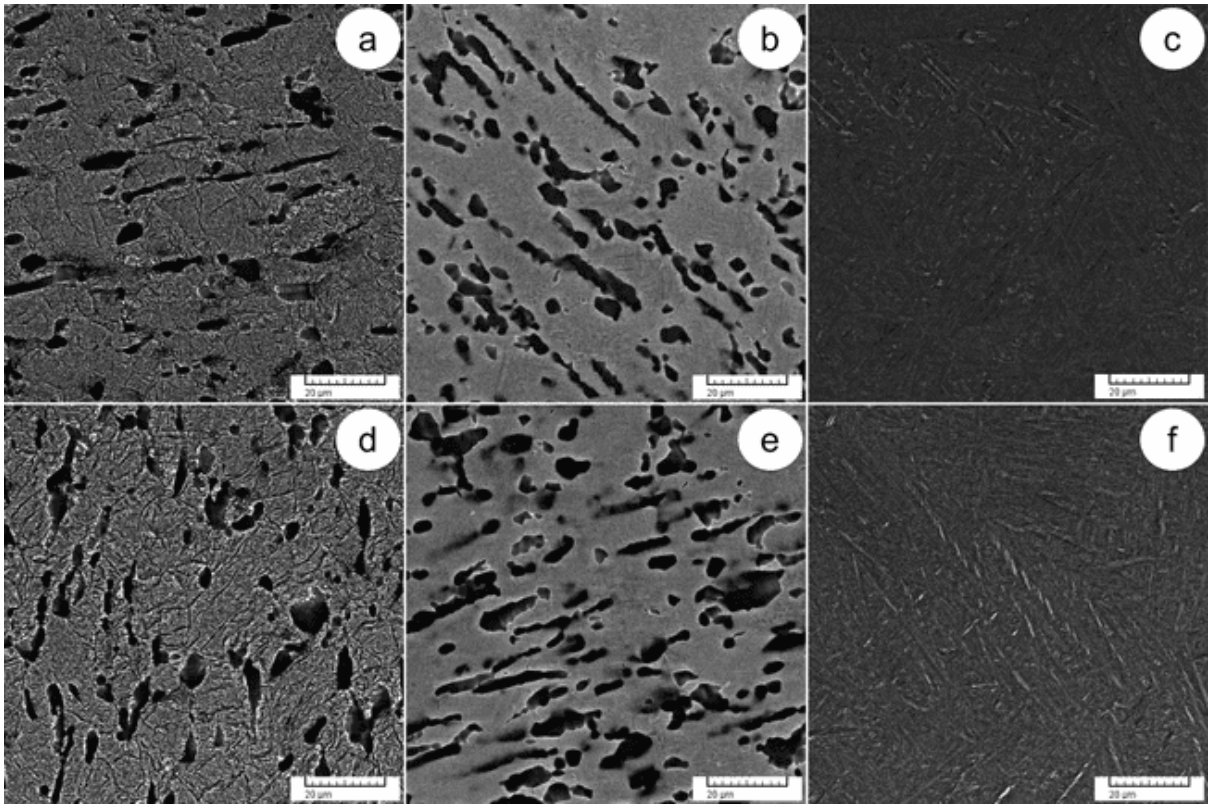

Fig. 7.4 *SEM-BSE images of ageing treatment at 600°C (A 1.2) case (a); ageing treatment at 600°C (A 3.2) case (b); ageing treatment at 600°C (A 5.2) case (c); ageing treatment at 600°C (A 2.2) case (d); ageing treatment at 600°C (A 4.2) case (e); ageing treatment at 600°C (A 6.2) case (f).*

The SEM-BSE images of the ST 2.1 + A 2.2 treatment case (see Fig. 7.4.d) display the same morphological character with the ST 2.1 treatment case consisting of the textural dispersion of the initial α-Ti and β-Ti phases. This textural dispersion includes the presence of colonies boundaries traces and random/irregular coarse morphologies of the initial α-Ti phase, in addition to the alternate thin lamellae/plate-like structures of the initial α-Ti and β-Ti phases showing a preferred spatial orientation. Treatment of ageing induces the secondary α'-Ti phase to transform to the initial α-Ti phase, meaning that the temperature and duration of ageing treatment are sufficient for these transformations to occur. The microstructure of the ST 4.1 + A 4.2 treatment case (see Fig. 7.4.e) shows the same morphological nature with the ST 4.1 treatment case about random/irregular coarse morphologies of the initial α-Ti phase dispersed within the β-Ti phase matrix with consideration of delicate-size for the lamellae/plate-like structures of initial α-Ti and β-Ti phases in the microstructure compared with the ST 4.1 treatment case. Also, the ageing treatment causes the secondary α'-Ti phase to transform to the initial α-Ti phase. Considering the ST 6.1 + A 6.2 treatment case (see Fig. 7.4.f), it can observe that the microstructure contains basket-weave type morphology, and structures of fine

lamellar/acicular beside large parallel platelets in size within the microstructure as a consequence of rapid cooling at a temperature of 1000°C to ambient temperature. Secondary α'-Ti/α''-Ti phases that originated inside the microstructure reverted to initial α-Ti/β-Ti phases during ageing treatment due to adequate conditions to ageing treatment.

7.2. Mechanical behaviour during thermomechanical processing

7.2.1. Mechanical properties evolution during thermomechanical processing

The recorded parameters of the mechanical properties: ultimate tensile strength (σ_{UTS}), 0.2% yield strength ($\sigma_{0.2\%}$), elongation to fracture (ε_f) during tensile testing and microhardness (HV1). Table 7.1 presents the values of the recorded parameters for the mechanical properties. The case of hot deformation presented a relatively large increase in microhardness, when compared with the condition of the as-received Ti-6246 alloy, due to the work-hardening mechanism, leading to the formation of defects within the microstructure, providing further hardening to the Ti-6246 alloy. In tensile testing, the strength properties (σ_{UTS} and $\sigma_{0.2\%}$) increased slightly in the case of hot deformation due to the effects of low deformation of the initial grains and the alternate lamellae/plate-like texture of the α-Ti phase embedded in the β-Ti phase matrix, while the ductility (ε_f) decreased significantly, as a result of the hardening of the material when compared with the condition of the as-received Ti-6246 alloy, confirming microstructural observations by SEM-BSE images.

A decrease in microhardness observes in the ST 1.1 and ST 2.1 treatment cases compared to the hot deformation case due to the decrease in defects density in the microstructure (stress-relieving phenomenon). At the solution temperature of 800°C (the ST 1.1 and ST 2.1 treatment cases), the microstructure includes initial α-Ti and β-Ti phases, and recrystallisation occurs only in α-Ti phase and β-Ti phase restructuring. During rapid cooling, the initial α-Ti phase generates the secondary α'-Ti phase, and the β-Ti phase does not have secondary phasic transformations. Therefore, the strength and ductility properties show a marked increase in tensile testing. The microhardness of the ST 3.1 and ST 4.1 treatment cases showed a marked decrease due to the lower defects density (stress-relieving phenomenon) compared to the cases of ST 1.1 and ST 2.1 treatment. At the solution temperature of 900°C (the ST 3.1 and ST 4.1 treatment cases), the initial α-Ti phase transformation to the secondary α'-Ti phase continues until the α'-Ti phase is of a higher fractional volume compared to prior treatments (ST 1.1 and ST 2.1 cases) beside the initial α-Ti and β-Ti phases in the alloy microstructure, increasing the properties of the strength and ductility in tensile testing (see Table 7.1). The microhardness increases slightly in the ST 5.1 and ST 6.1 treatment cases compared to the ST 3.1 and ST 4.1 treatment cases, because of the dispersion of the secondary α''-Ti phase particles in the β-Ti phase matrix, within the microstructure of Ti-6246 alloy, increasing the hardening of the material. At the solution temperature of 1000°C (the ST 5.1 and ST 6.1 treatment cases), the microstructure is in the single β-Ti phase. During the rapid cooling, the secondary α''-Ti phase generated from the initial β-Ti phase, and β-Ti $\rightarrow$ α-Ti $\rightarrow$ α'-Ti transformations can induce in the microstructure. The mechanical properties significantly affected due to the α''-Ti phase precipitation, as strength properties decreased and ductility increased in tensile testing.

Table 7.1

Recorded mechanical properties for processed Ti-6246 alloy in the second experimental program

Structural state	Mechanical properties

	Microhardness, HV1	Ultimate tensile strength, σ_{UTS} [MPa]	0.2 yield strength, $\sigma_{0.2\%}$ [MPa]	Elongation to fracture, ε_f [%]
As-received (**AR**)	305.2±16.9	1057±14	967±11	12.9±1.8
Hot-deformed at 900°C (**HD2**)	399.8±13.7	1154±14	996±13	3.8±0.8
Solution treatment: T = 800°C; t = 9min/3mm; OQ (**ST1.1**)	373.5±5.4	1165±13	1008±12	5.3±1.1
Solution treatment: T = 800°C; t = 18min/3mm; OQ (**ST2.1**)	354.3±8.9	1221±12	1071±14	5.8±0.9
Solution treatment: T = 900°C; t = 9min/3mm; OQ (**ST3.1**)	301.8±5.8	1357±14	1174±12	6.9±1.2
Solution treatment: T = 900°C; t = 18min/3mm; OQ (**ST4.1**)	291.6±9.2	1395±11	1184±12	7.2±1.1
Solution treatment: T = 1000°C; t = 9min/3mm; OQ (**ST5.1**)	320.4±5.9	984±13	785±13	9.7±1.2
Solution treatment: T = 1000°C; t = 18min/3mm; OQ (**ST6.1**)	306.8±8.1	1074±10	844±11	10.4±1.4
ST1.1 + Ageing treatment: T = 600°C; t = 6h; AQ (**A1.2**)	397.8±9.1	1089±11	966±13	8.1±1.3
ST2.1 + Ageing treatment: T = 600°C; t = 6h; AQ (**A2.2**)	402.2±5.7	1088±13	959±10	8.3±1.4
ST3.1 + Ageing treatment: T = 600°C; t = 6h; AQ (**A3.2**)	428.1±5.3	1284±12	1101±14	15.4±1.2
ST4.1 + Ageing treatment: T = 600°C; t = 6h; AQ (**A4.2**)	430.1±5.5	1289±10	1097±12	15.6±1.3
ST5.1 + Ageing treatment: T = 600°C; t = 6h; AQ (**A5.2**)	442.6±3.7	1170±11	986±13	6.9±1.2
ST6.1 + Ageing treatment: T = 600°C; t = 6h; AQ (**A6.2**)	454.2±6.7	1176±13	992±11	7.1±1.4

The ST 1.1 + A 1.2 and ST 2.1 + A 2.2 treatment cases experienced a slight increase in microhardness compared to the ST 1.1 and ST 2.1 treatment cases due to the applied ageing treatment. On the other hand, the treatment cases (ST 1.1 + A 1.2 and ST 2.1 + A 2.2) showed a decrease in tensile testing strength properties and an increase in ductility due to the return of the secondary α'-Ti phase to the initial α-Ti phase, giving this effect on mechanical properties compared to the treatment cases (ST 1.1 and ST 2.1). In the ST 3.1 + A 3.2 and ST 4.1 + A 4.2 treatment cases, the microhardness increased significantly compared with the ST 3.1 and ST 4.1 treatment cases under the ageing treatment conditions. In tensile testing, a large decrease in strength properties observed in the ST 3.1 + A 3.2 and ST 4.1 + A 4.2 treatment cases compared with the cases of ST 3.1 and ST 4.1 treatment and the ductility property with the highest fracture elongation among thermomechanical processing cases. The reason for this decrease in strength properties of tensile testing is due to sufficient conditions for ageing treatment transforming the secondary α'-Ti phase to the initial α-Ti phase, reducing the strength of the material. The cases of ST 5.1 + A 5.2 and ST 6.1 + A 6.2 treatment showed a considerable increase in microhardness compared to the ST 5.1 and ST 6.1 treatment cases, the reason may be the probability of generating α-Ti/ω-Ti phase particles in the β-Ti phase matrix inside the microstructure of Ti-6246 alloys, and these particles provide further hardening to the material. In tensile testing, the cases of ST 5.1 + A 5.2 and ST 6.1 + A6.2 treatment showed a large increase in strength properties and a large decrease in ductility property compared to the ST 5.1 and ST 6.1 treatment cases. Although the absence of the secondary α''-Ti phase, the probability of very fine precipitates in nanometer-sized in the β-Ti phase generated from the α-

Ti/ω-Ti phase is possible, serving to strengthen the material behaviour (age hardening mechanism).

7.2.2. Fracture surfaces analysis of thermomechanical processed cases

Depending on the examination of the fracture surfaces obtained after tensile testing, one can assess the fracture behaviour of the Ti-6246 alloy induced by the effect of the application of the thermomechanical processing route on the tested samples.

7.2.2.1. Fracture surfaces analysis of as-received (AR) and hot deformation (HD2) cases

Fig. 7.5 shows images of fracture surfaces obtained at different magnifications for the as-received (AR) Ti-6246 alloy (Fig. 7.5.a and b) and the hot deformation (HD2) case at 900°C (Fig. 7.5.c and d).

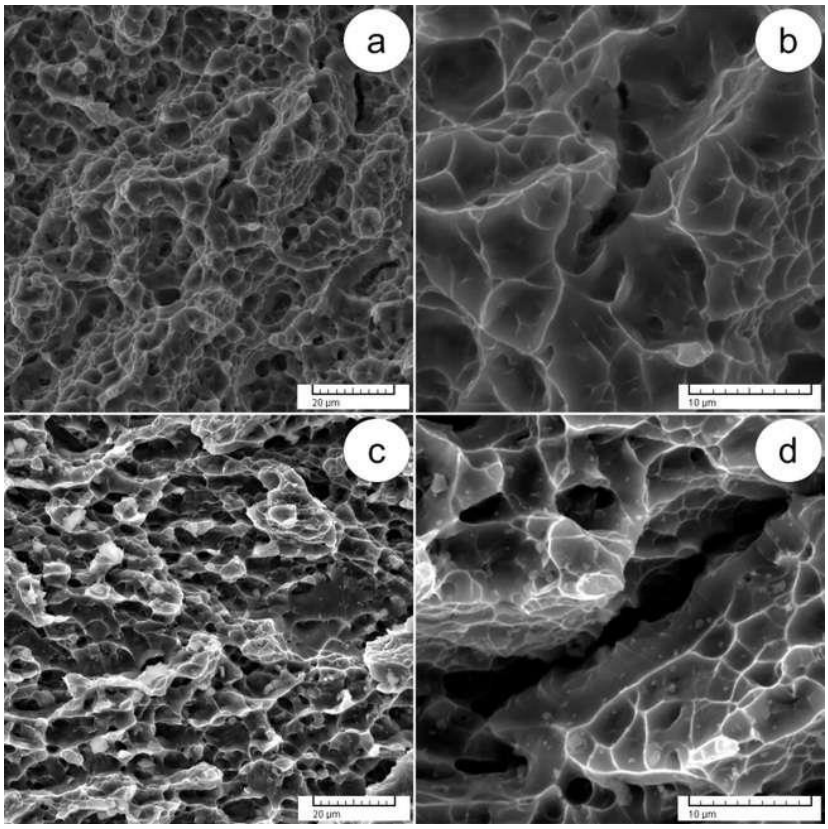

Fig. 7.5 *SEM-SE images of fracture surfaces after tensile testing of Ti-6246 alloy in AR case in different magnifications (a and b); HD2 case in different magnifications (c and d).*

In the analysis of AR alloy, the fracture surfaces show a spongy morphology, having a high density of voids and dimples (Fig. 7.5.a), showing an obvious ductility, as noticed, the presence of the voids coalescence mechanism (Fig. 7.5.b). Overall, the AR alloy shows ductile behaviour, confirming mechanical observations (high strength of 1057±14MPa and high elongation to fracture of 12.9±1.8%). In the case of the hot-deformed (HD2) sample at a temperature of 900°C, the spongy areas are present next to the areas of dense small crevices/fissures and cleavage surfaces. The spongy areas include small voids and shallow dimples of lower density comparing with the as-received alloy (Fig. 7.5.c). The voids coalescence areas (Fig. 7.5.d) indicate the boundaries of prior deformed α-Ti and β-Ti colonies. Overall, the case of HD2 shows a mixture of brittle-ductile behaviour, confirming mechanical observations (moderate strength of 1154±14MPa and low elongation to fracture of 3.8±0.8%).

7.2.2.2. Fracture surfaces analysis of solution treatment (ST) cases

Fig. 7.6 presents typical SEM-SE micrographics of solution-treated (ST) fracture surfaces of Ti-6246 alloy at different temperatures and durations. Morphological observations of fracture surfaces in the case of ST 1.1 treatment (see Fig. 7.6.a) reveal the presence of small cleavage surfaces/areas and small crevices/fissures adjacent to the spongy areas containing small-sized voids and shallow dimples. Through these morphological observations (cleavage surfaces, crevices/fissures and spongy areas), the ST 1.1 treatment case shows limited ductility and possesses a mixed behaviour of brittle and ductile. SEM-SE micrographics of the ST 3.1 treatment case (see Fig. 7.6.b) show morphological observations almost similar to the case of ST 1.1 treatment, but with higher-size cleavage surfaces and less dense spongy areas. The spongy areas also have small-size voids and shallow dimples, as in the case of ST 1.1, presenting a low/limited ductility (fracture elongation) and a mixed behaviour of brittle and ductile in the case of ST 3.1 treatment. The morphological appearances observed for the fracture surfaces in the ST 5.1 treatment case (see Fig. 7.6.c) are predominantly large cleavage surfaces, and the spongy areas are minimal and still contain small-sized voids and shallow dimples. Overall, the ST 5.1 treatment case exhibits an obvious brittle behaviour and moderate ductility, supporting the observations in the analysis of mechanical properties (moderate strength of 984±13MPa and elongation to fracture of 9.7±1.2%).

Analysing the fracture surface of the ST 2.1 treatment case (see Fig. 7.6.d), one can observe the presence of small cleavage surfaces/areas and small crevices/fissures adjacent to the spongy areas. The spongy areas contain small-sized voids and shallow dimples, and one of the small crevices/fissures is also clearly visible. According to the morphological observations (cleavage surfaces, crevices/fissures and spongy areas), one can see that the ST 2.1 treatment case has limited ductility and possesses a mixed behaviour of brittle and ductile. In the analysis of the fracture surface of the ST 4.1 treatment case (see Fig. 7.6.e), the morphological features show large cleavage surfaces with higher density and spongy areas with lower density compared to the ST 2.1 treatment case, also observed that the spongy areas contain shallow dimples and voids of small size being minimal, confirming low/limited ductility (fracture elongation), and this case shows a mixed behaviour of brittle and ductile. Considering the case of ST 6.1 treatment (see Fig. 7.6.f), one can observe that the fracture surface predominantly includes large cleavage surfaces, and spongy areas at minimal, as these areas contain small-sized voids and shallow dimples compared to the cases of ST 2.1 and ST 4.1 treatment. Overall, the case of ST 6.1 treatment shows by morphological observations a pronounced brittle behaviour and a moderate ductility, confirming the mechanical properties investigation observations (moderate strength of 1074±10MPa and elongation to fracture of 10.4±1.4%).

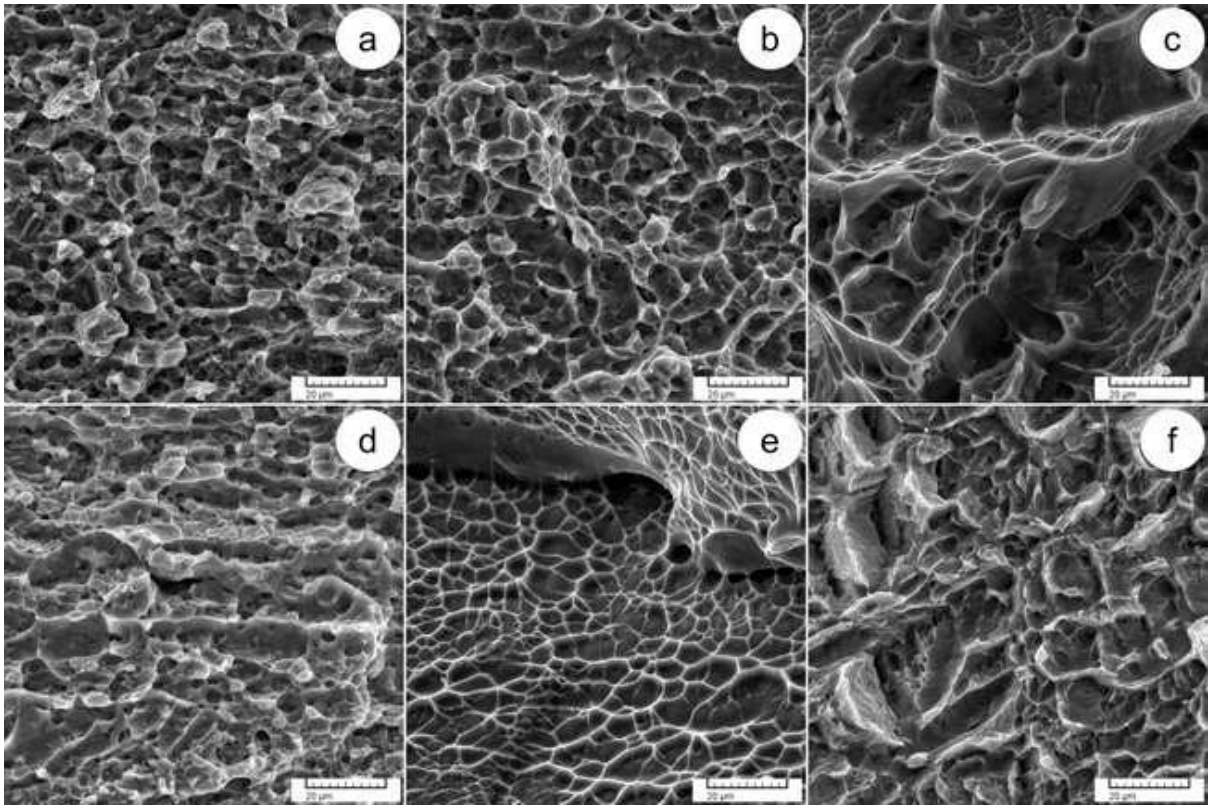

Fig. 7.6 *SEM-SE images of fracture surfaces after tensile testing of Ti-6246 alloy in (ST 1.1) case (a); (ST 3.1) case (b); (ST 5.1) case (c); (ST 2.1) case (d); (ST 4.1) case (e); (ST 6.1) case (f).*

7.2.2.3. Fracture surfaces analysis of ageing (A) cases

Fig. 7.7 presents typical SEM-SE micrographics of ageing-treated (A) fracture surfaces of Ti-6246 alloy at constant temperature and duration after solution treatment (ST). By noticing the fracture surfaces in the case of ST 1.1 + A 1.2 treatment (see Fig. 7.7.a), morphological observations show the cleavage surfaces and crevices/fissures of small sizes adjacent to the spongy areas. In the spongy areas, the voids are small, and the dimples are shallow, concluding that the ductility is limited, and this is consistent with the observations of the mechanical investigation, giving the mixed behaviour of the brittle and ductile type in the case of ST 1.1 + A 1.2 treatment. Considering the fracture surface in the ST 3.1 + A 3.2 treatment case (see Fig. 7.7.b), one can observe that the cleavage surfaces are of lower density compared with the ST 3.1 and ST 1.1 + A1.2 treatment cases and are small in size located adjacent to the spongy areas and these spongy areas have shallow dimples and small-sized voids with higher intensity compared with the ST 3.1 and ST 1.1 + A1.2 treatment cases, one can conclude that the case of ST 3.1 + A 3.2 treatment possesses high ductility based on morphological observations presented in line with mechanical observations. The fracture surface of the ST 5.1 + A 5.2 treatment case (see Fig. 7.7.c) shows small cleavage surfaces compared to the ST 5.1 treatment case and the spongy areas at a minimum compared to the ST 1.1 + A 1.2 and ST 3.1 + A 3.2 treatment cases. Inside the spongy areas, the voids are small, the dimples are shallow, and the voids coalescence areas are also observed, indicating lower ductility and higher strength compared to the ST 5.1 treatment case, and the reason can be attributed to the dispersion of strengthening particles of the α-Ti/ω-Ti phase within the β-Ti phase, conferring this behaviour on the material and this is compatible with the mechanical observations that discussed before.

Morphological observations of ST 2.1 + A 2.2 treatment case (see Fig. 7.7.d) present small sizes of cleavage surfaces and crevices/fissures next to the spongy areas. Within the spongy areas, one can notice small-sized voids, shallow dimples and voids coalescence, allowing for limited ductility, as mentioned in mechanical observations, and the ST 2.1 + A 2.2 treatment case presents a mixed behaviour of the brittle and ductile type. In the ST 4.1 + A 4.2 treatment case (see Fig. 7.7.e), morphological observations of the fracture surface show the presence of small-sized cleavage surfaces of lower density when compared with the ST 4.1 and ST 2.1 + A 2.2 treatment cases next to the spongy areas. The spongy areas include small-sized voids and shallow dimples with a higher density in comparison with the ST 4.1 and ST 2.1 + A 2.2 treatment cases, and according to the morphological observations, the ST 4.1 + A 4.2 treatment case revealed a high ductility harmonised with the mechanical observations. In the case of ST 6.1 + A 6.2 treatment (see Fig. 7.7.f), it can observe that the cleavage surfaces are small in size and have a lower density compared to the case of ST 6.1 treatment and the spongy areas being at a minimum when compared with the cases of ST 2.1 + A 2.2 and ST 4.1 + A 4.2 treatment. In the spongy areas, one can observe shallow dimples, small-sized voids, and voids coalescence areas, showing lower ductility and higher strength, compared to the ST 6.1 treatment case, and this behaviour may be due to precipitation of strengthening particles of α-Ti/ω-Ti phase inside β-Ti phase, supporting the aforementioned mechanical observations.

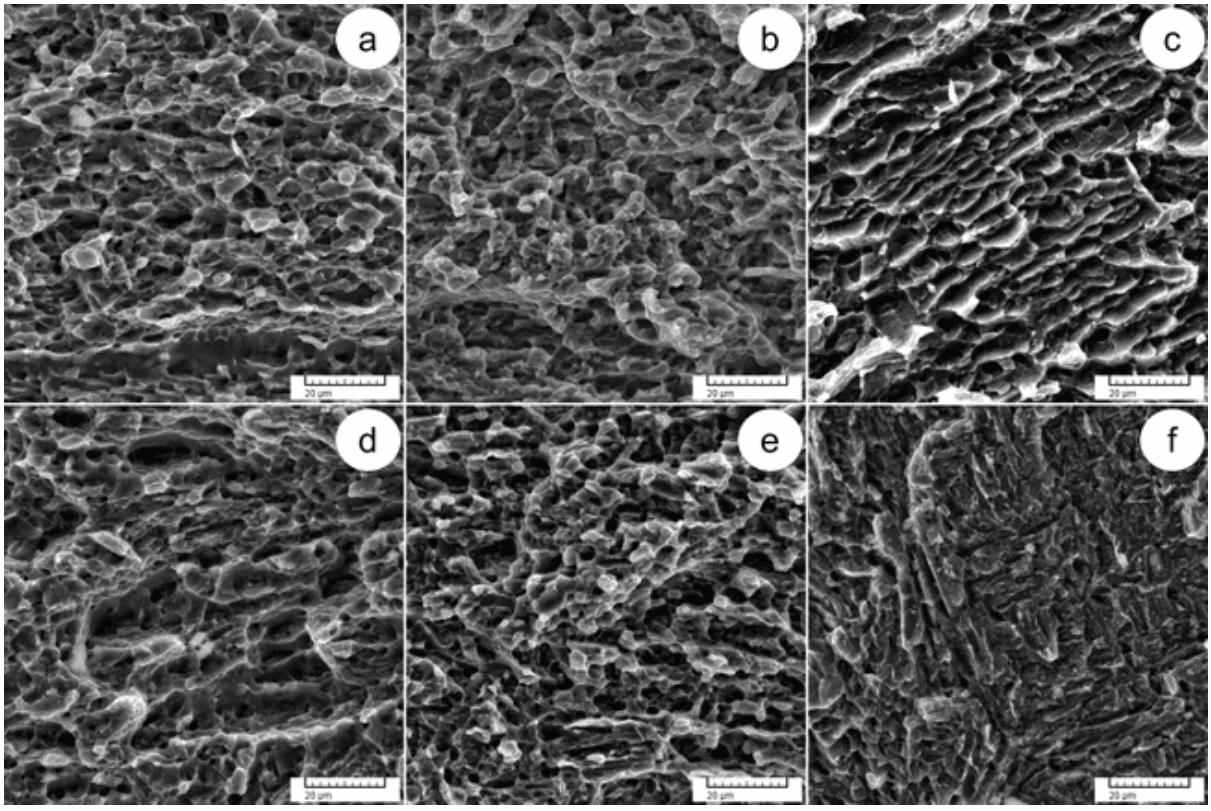

Fig. 7.7 *SEM-SE images of fracture surfaces after tensile testing of Ti-6246 alloy in (A 1.2) case (a); (A 3.2) case (b); (A 5.2) case (c); (A 2.2) case (d); (A 4.2) case (e); (A 6.2) case (f).*

7.3. Conclusions

The evolution of the microstructure and mechanical properties studied of Ti-6246 alloy during different thermomechanical processing steps. The processing route includes a microstructure

deformation step below the β-transus temperature at 900°C followed by solution and ageing treatments steps to assess the structural and mechanical behaviours resulting from this processing route. The following conclusions can summarise as follows:

- At the solution temperature of 800°C, the ductility increases, and the secondary α'-Ti phase is generated within the microstructure, increasing the strength properties compared to hot deformation (HD2) case, while at the solution temperature of 900°C, the secondary α'-Ti phase continues to appear within the microstructure beside the increase in the volumetric fraction of the β-Ti phase, increasing the strength and ductility properties compared to the hot deformation (HD2) case and solution treatment cases performed at 800°C.
- At the solution temperature of 1000°C, the secondary α''-Ti phase is generated from the initial β-Ti phase within the microstructure, and strength properties decrease compared to the HD2 case and solution treatment cases performed at 800°C and 900°C, while ductility increases compared to the HD2 case and solution treatment cases performed at 800°C and 900°C due to the treatment performed in the β-Ti phase field.
- The cases of solution treatment performed at temperatures of 800°C, 900°C and 1000°C with treatment duration of 18mins and rapid cooling showed an increase in the strength and ductility properties compared to the cases of solution treatment performed under the same conditions but with treatment duration of 9mins.
- Significant changes occurred during the ageing treatment concerning (α'-Ti/α''-Ti → α-Ti/β-Ti and β-Ti → α-Ti/ω-Ti) phasic transformations and the phenomena of stress-relieving and ageing-hardening. The performed ageing treatment at a temperature of 600°C with a treatment duration of 6h and air quenching after the solution treatments performed below β-transus temperature (at 800°C and 900°C) with different treatment durations showed a decrease in the strength properties and an increase in the ductility property compared to solution treatment cases, especially in the performed ageing treatment after solution treatment close to β-transus temperature (≈ 935°C) showing the highest ductility. On the other hand, the performed ageing treatment at a temperature of 600°C with treatment duration of 6h and air quenching after the solution treatment performed above β-transus temperature (at 1000°C) with different treatment durations showed an increase in the strength properties and a decrease in the ductility property compared to solution treatment cases.
- Ageing treatment may slightly decrease the strength or ductility properties, but without ageing treatment, this balance in mechanical properties cannot achieve, where it strives to provide a better combination of strength and ductility properties.

Chapter 8: Results and discussion (Experimental program III)

8.1. Microstructure evolution during thermomechanical processing

8.1.1. Microstructure analysis of hot deformation (HD3) case

Fig. 8.1 shows typical SEM-BSE microstructural images at different magnifications and XRD spectra image of hot-deformed (HD3) Ti-6246 alloy. One can observe that the initial grains are heavily deformed, showing elongated morphology along the RD, and it is possible to give the same observation in the case of the grain's boundary, which tends to align along the RD (see Fig. 8.1.a). Due to high deformation temperature of 1000°C (above β-transus = 935°C) and high applied deformation (total deformation degree ≈ 60%), the adjacent α-Ti/β-Ti colonies are intensely deformed, showing an elongated morphology, with an average thickness close to 15µm. Deformed α-Ti/β-Ti colonies separate with thin boundaries, which appear due to the applied intense deformation and the difference in initial spatial orientation of α-Ti/β-Ti colonies (see Fig. 8.1.b). The XRD spectra of HD-3 state (see Fig. 8.1.c) shows that the diffraction peaks of both α-Ti and β-Ti phases are characterised by large widths (peak broadening), indicating a low grain-size for both α-Ti and β-Ti phases.

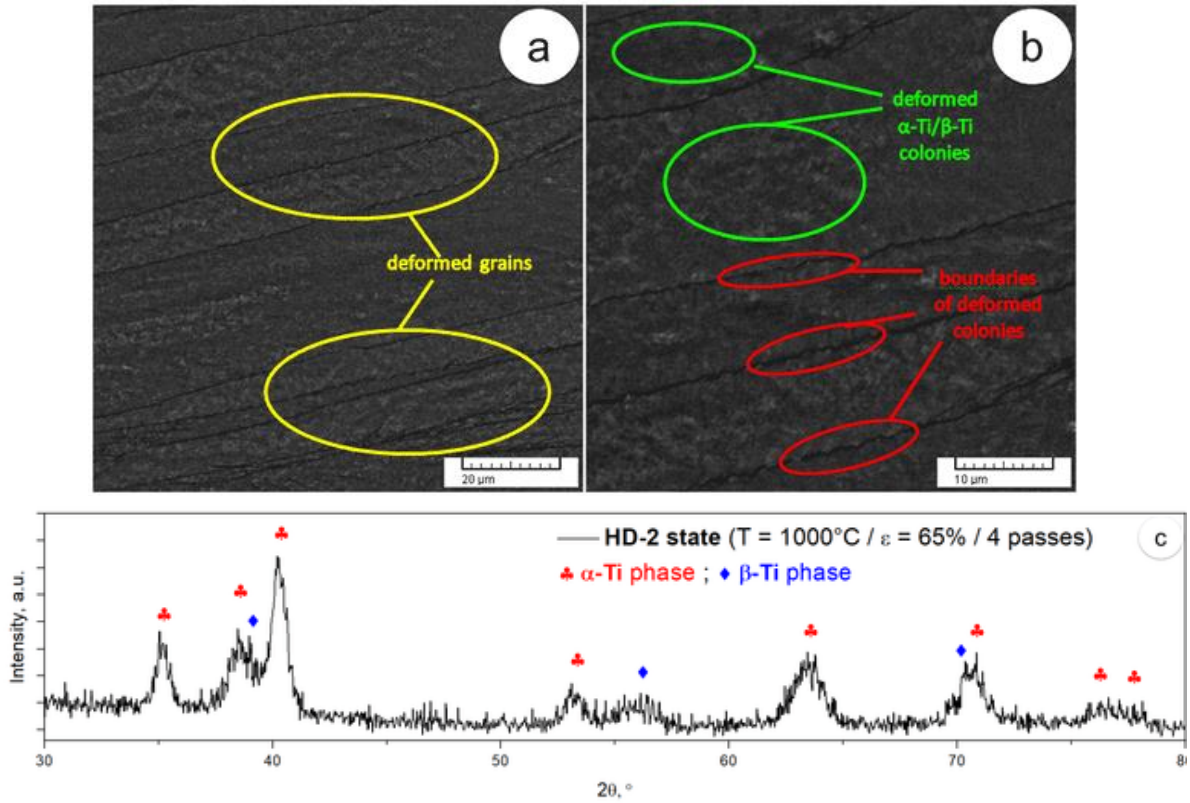

Fig. 8.1 *SEM-BSE images of hot-deformed (HD3) case in different magnifications (a and b); XRD spectra of HD3 case (c).*

8.1.2. Microstructure analysis of solution treatment (ST) cases

Fig. 8.2 shows typical SEM-BSE microstructural images of solution treated (ST) Ti-6246 alloy at different temperatures and durations. In the case of ST 7.1 treatment (see Fig. 8.2.a), performed well below the β-transus temperature (≈ 935°C), one can observe that the heavily deformed grains fully recrystallised, but one can notice the presence of boundaries traces of prior deformed colonies. Both α-Ti and β-Ti phases fully regenerated as alternate thin lamellae/plate-like structures showing preferred spatial orientation. Besides α-Ti and β-Ti phases, one can notice the presence of a dispersed fine acicular phase, identified as α'-Ti phase,

generated due to rapid cooling at ambient temperature. The α'-Ti phase shows a preferred orientation with the parent α-Ti phase due to the special Burgers relation between α-Ti/α'-Ti phases. In the case of ST 9.1 treatment (see Fig. 8.2.b), performed below close to the β-transus temperature (≈ 935°C), one can observe that the heavily deformed grains have fully recrystallised, generating a basket-weave -type morphology. The basket-weave morphology shows interconnected/parallel α-Ti/β-Ti lamellae presence, showing higher thickness lamellae when comparing to ST 7.1 state. When comparing the average thickness of α-Ti with a β-Ti lamella, one can observe that the α-Ti lamella shows a much higher thicker, suggesting that the heating to ST 9.1 treatment temperature favours recrystallisation of α-Ti phase. Also, one can notice inside α-Ti lamella the presence of α'-Ti phase, which shows a platelet-like morphology. The α'-Ti phase is generated due to rapid cooling at ambient temperature. Analysing the case of ST 11.1 treatment (see Fig. 8.2.c), performed above β-transus temperature (≈ 935°C), one can observe that the microstructure shows, also, a basket-weave -type morphology. The rapid cooling from 1000°C to ambient temperature induces the formation of a microstructure consisting of a mixture of lamellar/acicular fine dispersion and larger parallel platelets. The parallel platelets were identified as α''-Ti phase and formed due to rapid cooling at the ambient temperature of the β-Ti phase. The α''-Ti phase shows preferred spatial orientation with the parent β-Ti phase due to the special Burgers relation between the β-Ti/α''-Ti phases.

Observations of ST 8.1 case treatment (see Fig. 8.2.d), performed well below the β-transus temperature (≈ 935°C), are full recrystallisation of heavily deformed grains with the presence of boundaries traces of prior deformed colonies and concomitant full regeneration to the texture of the initial α-Ti and β-Ti phases with structures similar to alternate thin lamellae/plate, which represents the preferred spatial orientation. The α'-Ti phase is observed with a fine-acicular structure generated as a result of rapid cooling and dispersed in the initial α-Ti phase in the same preferred orientation of the initial α-Ti phase texture. In the treatment of ST 10.1 case (see Fig. 8.2.e), performed below close to the β-transus temperature (≈ 935°C), one can see full recrystallisation of heavily deformed grains with the lamellar texture of the α-Ti and β-Ti phases combined in parallel in directions spatially intersected to form a morphology similar to basket-weave -type. This lamellar texture with a basket-weave -type morphology shows a higher thickness when compared to the thickness of the lamellar texture in the case of ST 8.1 treatment, indicating that the treatment close to the β-transus temperature preferred for recrystallisation in the texture of α-Ti phase more than the texture of β-Ti phase. Moreover, the α'-Ti phase with a fine platelet-like morphology generated from the α-Ti phase can observe during rapid cooling at ambient temperature. In the case of ST 12.1 treatment (see Fig. 8.2.f), performed above β-transus temperature (≈ 935°C), the microstructure is observed to have a morphology with the basket-weave -type. It also observed that the microstructure is composed of fine lamellar/acicular and large parallel platelets structures. Formation of α''-Ti phase with large parallel platelets resulting from rapid cooling at 1000°C in the β-Ti phase field to ambient temperature. The dispersion of this phase in the initial β-Ti phase shows the preferred spatial orientation of this phase according to Burgers relation between β-Ti/α''-Ti phases.

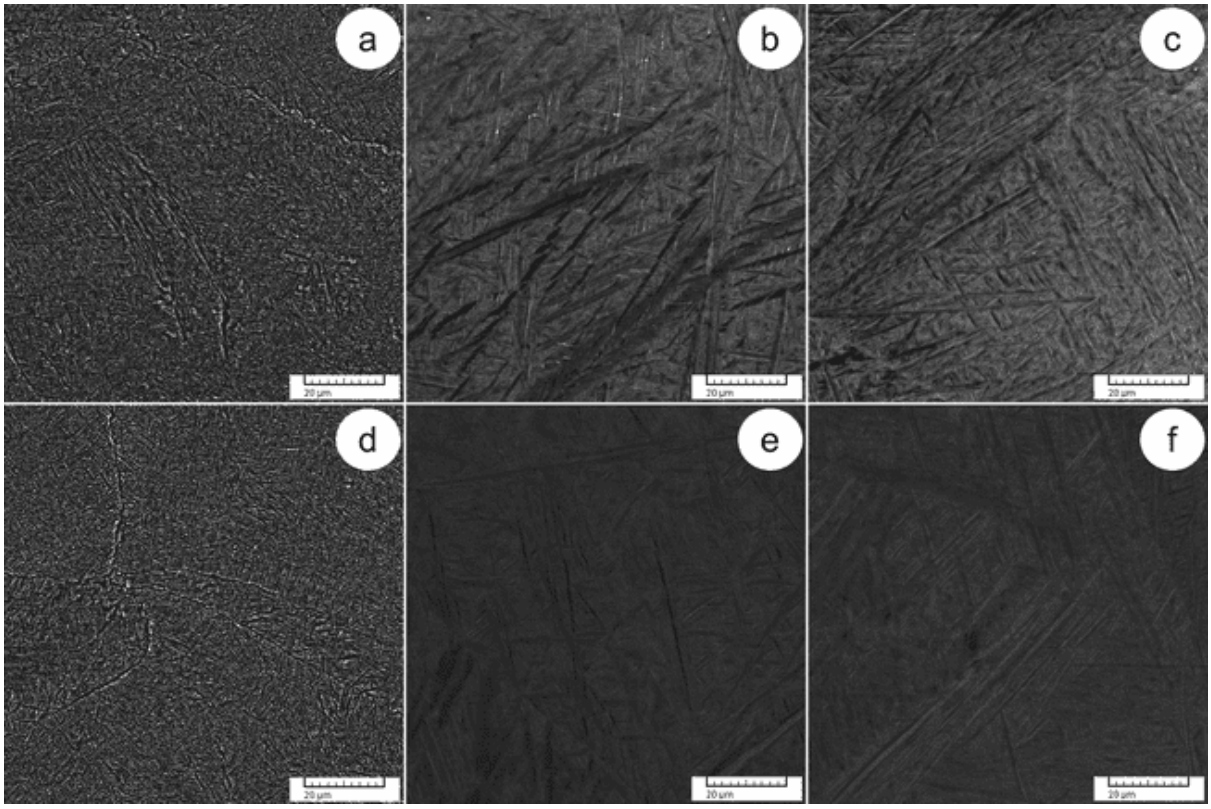

Fig. 8.2 *SEM-BSE images of solution treatment at 800°C (ST 7.1) case (a); solution treatment at 900°C (ST 9.1) case (b); solution treatment at 1000°C (ST 11.1) case (c); solution treatment at 800°C (ST 8.1) case (d); solution treatment at 900°C (ST 10.1) case (e); solution treatment at 1000°C (ST 12.1) case (f).*

Fig. 8.3 shows typical XRD spectra of solution treated (ST) states at different temperatures. In the case of ST 7.1 treatment, performed well below the β-transus temperature (≈ 935°C), one can observe diffraction peaks belonging to β-Ti, α-Ti and α'-Ti phases (see Fig. 8.3.a). The β-Ti phase classifies in the BCC crystalline system, with lattice parameters close to a = 0.327nm. The α-Ti and α'-Ti phases classify in the HCP crystalline system, and both show close lattice parameters (close to a = 0.294nm and c = 0.467nm), and thus difficult to distinguish between them. The differences in lattice parameters are due to supersaturation in β-stabilizers elements in the α''-Ti phase compared to the α-Ti phase. In the case of ST 9.1 treatment, performed below close to the alloy transition temperature (≈ 935°C), one can see diffraction peaks belonging to β-Ti, α-Ti and α'-Ti phases (see Fig. 8.3.b). Analysing the relative intensities of diffraction peaks, one can see the tendency of the phase texture along certain crystallographic directions, suggesting the preferred growth of crystallographic grains at all phases, supporting SEM-BSE microstructural observations (see Fig. 8.2.b). In the ST 11.1 treatment case, performed above the β-transus temperature (≈ 935°C), one can observe diffraction peaks belonging to the α-Ti, β-Ti, α''-Ti phases and possibly α'-Ti phase (see Fig. 8.3.c). Due to the heating at 1000°C, i.e. in the β-Ti phase-field, during rapid cooling to ambient temperature, the α''-Ti phase is generated. The α''-Ti phase classifies in the orthorhombic crystalline system, with lattice parameters close to a = 0.296nm, b = 0.496nm and c = 0.468nm. Due to the close lattice parameters of both α-Ti and α'-Ti phases, during analysis, only the α-Ti phase was considered. Analysing the relative intensities of diffraction peaks, one can notice texture directions showing the preferred growth of all phases within crystallographic grains, supporting

SEM-BSE microstructural observations (see Fig. 8.2.c). In all cases, if one analyses the width of the diffraction peaks (peaks broadening) can see that the peaks indicate low-sized grains for all observed phases, supporting SEM-BSE microstructural observations (see Fig. 8.2.a - c).

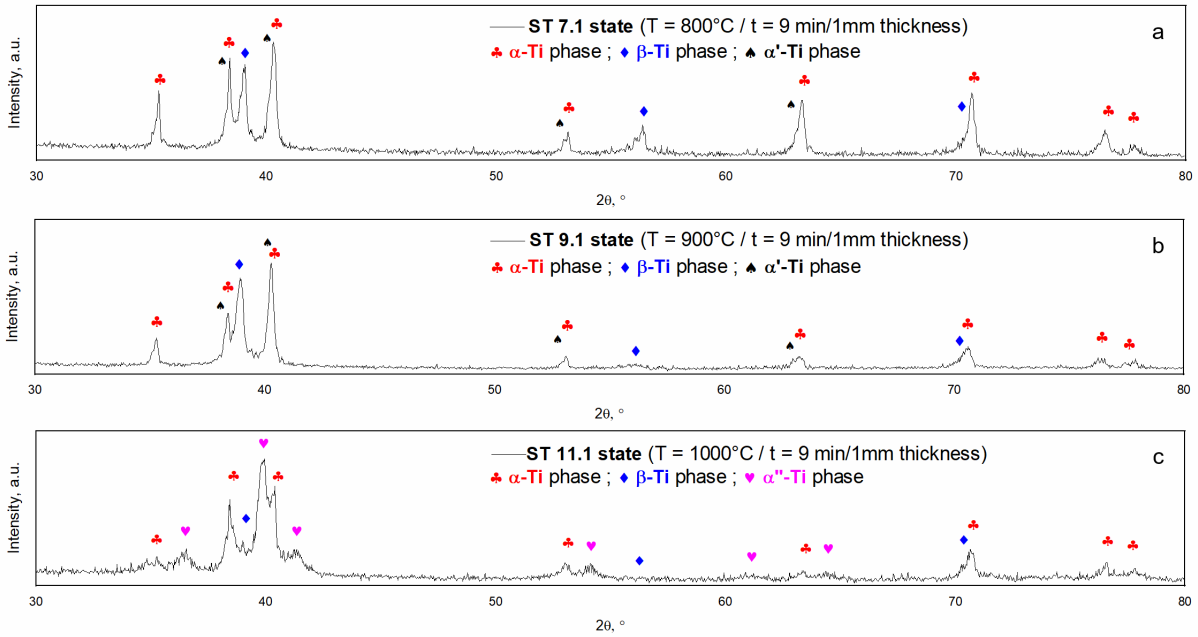

Fig. 8.3 *XRD spectra of solution treatment at 800°C (ST 7.1) case (a); solution treatment at 900°C (ST 9.1) case (b); solution treatment at 1000°C (ST 11.1) case (c).*

8.1.3. Microstructure analysis of ageing (A) cases

Fig. 8.4 shows typical SEM-BSE microstructural images of ageing treated (A) Ti-6246 alloy at fixed temperature and duration after solution treatment (ST). The microstructure of the ST 7.1 + A 7.2 treatment case (see Fig. 8.4.a) shows the same morphological approach compared to the ST 7.1 treatment case containing alternate thin lamellae/plate-like structures of α-Ti and β-Ti phases, besides the absence/degradation of the α'-Ti phase possessing fine acicular texture during the ageing treatment, confirming that the ageing temperature performed at 600°C with a treatment duration of 6h is sufficient to induce the secondary α'-Ti phase transformation to the initial α-Ti phase. In the case of ST 9.1 + A 9.2 treatment (see Fig. 8.4.b), it is possible to observe the traces of recrystallised colonies boundaries and the microstructure containment of a mixture of thick lamellar/plates of large and small sizes dispersed within the β-Ti phase matrix. Also, The dispersion of the globular-like morphology of the α-Ti phase is clearly visible within the β-Ti phase matrix, and ageing treatment caused the α'-Ti phase degradation and its transformation to the α-Ti phase, i.e., the α'-Ti phase did not observe in the microstructure. The SEM-BSE images of the ST 11.1 + A 11.2 treatment case (see Fig. 8.4.c) show that the microstructure possesses a basket-weave type morphology and includes structures similar to the alternate thin lamellae/plate of α-Ti and β-Ti phases. One can notice that ageing treatment resulted in the transformation of α'-Ti/α''-Ti phases into α-Ti/β-Ti phases, i.e. no traces of α'-Ti/α''-Ti phases were observed in the microstructure.

Analysing the case of ST 8.1 + A 8.2 treatment (see Fig. 8.4.d), one can see the same morphological concept consisting of alternate thin lamellae/plate structures of α-Ti and β-Ti phases as in the ST 8.1 treatment case, and can also see the traces of recrystallised colonies boundaries. The modification of the microstructure can observe by observing that the α'-Ti

phase possessing a fine acicular structure is no longer observed due to sufficient ageing treatment conditions to transform the α'-Ti phase to the α-Ti phase. In the case of the ST 10.1 + A 10.2 treatment (see Fig. 8.4.e), it can detect boundaries traces of recrystallised colonies and the microstructure possessing alternate thick lamellar/plates of the α-Ti phase in the β-Ti phase matrix. Besides, it is possible to observe the morphological appearance similar to the globular-type of α-Ti phase dispersed in the β-Ti phase matrix. The ageing treatment induces the transformation of the secondary α'-Ti phase into the initial α-Ti phase, indicating that ageing treatment conditions are sufficient to complete this transformation. Observations in SEM-BSE images of the ST 12.1 + A 12.2 treatment case (see Fig. 8.4.f) indicate the presence of a basket-weave type morphology and fine dispersion of the lamellae/plate-like structures of the α-Ti and β-Ti phases. Moreover, the ageing treatment served to degrade the secondary α'-Ti and α''-Ti phases and returned to the initial α-Ti and β-Ti phases due to the adequate conditions applied to the Ti-6246 alloy, i.e., no visible hints of the α'-Ti and α''-Ti phases.

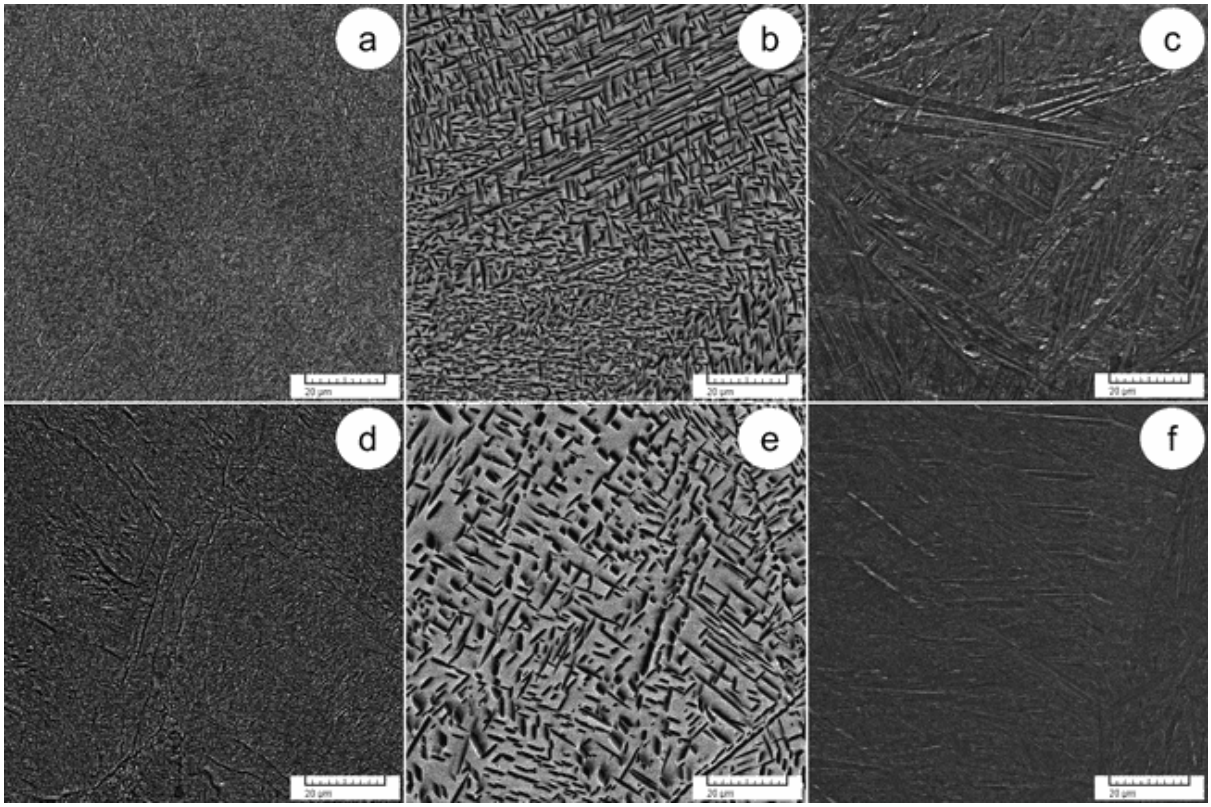

Fig. 8.4 *SEM-BSE images of ageing treatment at 600°C (A 7.2) case (a); ageing treatment at 600°C (A 9.2) case (b); ageing treatment at 600°C (A 11.2) case (c); ageing treatment at 600°C (A 8.2) case (d); ageing treatment at 600°C (A 10.2) case (e); ageing treatment at 600°C (A 12.2) case (f).*

8.2. Mechanical behaviour during thermomechanical processing

8.2.1. Mechanical properties evolution during thermomechanical processing

The following mechanical properties considered: ultimate tensile strength (σ_{UTS}), 0.2% yield strength ($\sigma_{0.2\%}$), elongation to fracture (ε_f) during tensile testing and microhardness (HV1). Table 8.1 presents the computed values of considered mechanical properties. A relatively large

increase in the property of microhardness (HV1) of the hot deformation case appeared compared to the as-received Ti-6246 alloy condition due to the work-hardening. A decrease in the strength (σ_{UTS} and $\sigma_{0.2\%}$) and ductility (ε_f) properties of the hot deformation case can also observe compared to the as-received Ti-6246 alloy. This decrease associate with the large deformation influences of the initial grains and the concomitant dense deformation for the similar texture to the alternate lamellae/plate of the α-Ti and β-Ti phases, leading to a high increase in the defects density within the alloy microstructure, thus increasing the material hardening due to less movement of defects and the material strengthening (work-hardening).

Table 8.1

Recorded mechanical properties for processed Ti-6246 alloy in the third experimental program

Structural state	Mechanical properties			
	Microhardness, HV1	Ultimate tensile strength, σ_{UTS} [MPa]	0.2 yield strength, $\sigma_{0.2\%}$ [MPa]	Elongation to fracture, ε_f [%]
As-received (**AR**)	305.2±16.9	1057±14	967±11	12.9±1.8
Hot-deformed at 1000°C (**HD3**)	417.8±6.1	1012±11	902±14	3.2±0.6
Solution treatment: T = 800°C; t = 9min/3mm; OQ (**ST7.1**)	385.1±10.1	1113±14	985±10	5.3±0.8
Solution treatment: T = 800°C; t = 18min/3mm; OQ (**ST8.1**)	351.2±4.7	1163±10	1021±12	5.8±0.7
Solution treatment: T = 900°C; t = 9min/3mm; OQ (**ST9.1**)	312.4±17.1	1205±12	1014±13	8.1±1.2
Solution treatment: T = 900°C; t = 18min/3mm; OQ (**ST10.1**)	299.7±12.5	1239±11	1055±11	8.2±0.9
Solution treatment: T = 1000°C; t = 9min/3mm; OQ (**ST11.1**)	339.8±21.3	961±12	747±15	7.2±0.9
Solution treatment: T = 1000°C; t = 18min/3mm; OQ (**ST12.1**)	304.5±10.6	998±11	794±12	7.8±1.1
ST7.1 + Ageing treatment: T = 600°C; t = 6h; AQ (**A7.2**)	325.2±11.9	1144±13	991±12	6.5±0.9
ST8.1 + Ageing treatment: T = 600°C; t = 6h; AQ (**A8.2**)	402.4±4.7	1057±10	908±10	6.5±1.0
ST9.1 + Ageing treatment: T = 600°C; t = 6h; AQ (**A9.2**)	425.2±4.5	1279±15	1161±14	10.1±1.3
ST10.1 + Ageing treatment: T = 600°C; t = 6h; AQ (**A10.2**)	437.8±11.5	1188±12	1038±12	10.5±1.1
ST11.1 + Ageing treatment: T = 600°C; t = 6h; AQ (**A11.2**)	442.6±9.6	1044±12	919±13	5.7±0.9
ST12.1 + Ageing treatment: T = 600°C; t = 6h; AQ (**A12.2**)	452.9±6.9	1096±14	955±11	5.9±1.0

One can see a decrease in the microhardness property in the cases of ST 7.1 and ST 8.1 treatments due to the stress-relieving phenomenon compared to the hot deformation (HR) case. The microstructure treated at 800°C consists of the initial α-Ti and β-Ti phases interweaving (the cases of ST 7.1 and ST 8.1 treatments), and the recrystallisation is only in the α-Ti phase, while the β-Ti phase is restructured during heating. The initial α-Ti phase generates the secondary α'-Ti phase, and there are no transformations in the β-Ti phase during rapid cooling. Accordingly, an increase in the strength (σ_{UTS} and $\sigma_{0.2\%}$) and ductility (ε_f) properties are observed. A notable decrease in microhardness property of the ST 9.1 and ST 10.1 treatments cases, as a consequence of the high effect of stress-relieving, compared to the cases of ST 7.1 and ST 8.1 treatments. In the treated microstructure at 900°C (ST 9.1 and ST 10.1 treatments cases), the initial α-Ti phase transformations continue to the secondary α'-Ti phase during rapid

cooling, making the α'-Ti phase possessing a higher fractional volume compared to the prior treatments (ST 7.1 and ST 8.1 cases) along with the α-Ti and β-Ti phases in the alloy microstructure, resulting in an increase in the properties of strength (σ_{UTS} and $\sigma_{0.2\%}$) and ductility (ε_f). The microhardness property of ST 11.1 and ST 12.1 treatment cases indicates a slight increase due to the presence of strengthening particles belonging to the secondary α''-Ti phase in the initial β-Ti phase matrix, meaning an increased hardening of the material compared with the ST 9.1 and ST 10.1 treatment cases. The microstructure is only in the β-Ti phase when treated at 1000°C (the cases of ST 11.1 and ST 12.1 treatment) as the HCP crystalline system belonging to the α-Ti phase transformed into the BBC crystalline system belonging to the β-Ti phase. Besides, during rapid cooling, the transformation from the initial β-Ti phase to the secondary α''-Ti phase takes place, and the β-Ti → α-Ti → α'-Ti transformations can induce in the alloy microstructure. The secondary α''-Ti phase significantly affected the mechanical properties, as properties of strength (σ_{UTS} and $\sigma_{0.2\%}$) and ductility (ε_f) decreased compared with the cases of ST 9.1 and ST 10.1 treatment.

The microhardness of the ST 7.1 + A 7.2 treatment case presented a decrease compared to the microhardness of the ST 7.1 treatment due to the stress-relieving phenomenon reducing the density of defects within the alloy microstructure and reduces the hardening of the material, while the increase in the microhardness of the ST 8.1 + A 8.2 treatment case compared to the microhardness of the ST 8.1 treatment because of the effect of ageing treatment. Considering the case of ST 7.1 + A 7.2 treatment, which shows a slight increase in the properties of strength (σ_{UTS} and $\sigma_{0.2\%}$) and ductility (ε_f) compared to the ST 7.1 treatment case as a result of the effects induced by the treatment of ageing and modification the microstructure (see Fig. 8.4.a), on the other hand when comparing the ST 8.1 + A 8.2 treatment case with the ST 8.1 treatment case, it experienced a decrease in strength (σ_{UTS} and $\sigma_{0.2\%}$) properties and an increase in ductility (ε_f) property due to the degradation of the fractional volume of the α′-Ti phase and its return to the α-Ti phase during ageing treatment (see Fig. 8.4.d). The microhardness property in the cases of ST 9.1 + A 9.2 and ST 10.1 + A 10.2 treatment increased significantly compared to the cases of ST 9.1 and 10.1 treatment, as a result of the application of ageing treatment. By seeing the case of ST 9.1 + A 9.2 treatment, properties of strength (σ_{UTS} and $\sigma_{0.2\%}$) and ductility (ε_f) increased when compared to the case of ST 9.1 treatment due to the induction of ageing treatment to refine alloy microstructure (see Fig. 8.4.b). Concerning the case of ST 10.1 + A 10.2 treatment, a slight decrease in strength (σ_{UTS} and $\sigma_{0.2\%}$) properties and an increase in ductility (ε_f) property can observe when compared to the case of ST 10.1 treatment based on the role that ageing treatment plays in the degradation of the α′-Ti phase and returned to the α-Ti phase along with the coarseness of the lamellar/plates structure in both cases (see Fig. 8.4.b and e), indicating the highest ductility value among thermomechanically processed cases. A significant increase in microhardness property is observed in the cases of ST 11.1 + A 11.2 and ST 12.1 + A 12.2 treatment compared to the ST 11.1 and ST 12.1 treatment cases. The reason attributed to the probability appearance of strengthening particles belonging to the α-Ti/ω-Ti phase dispersed in the β-Ti phase matrix. What is also observed in the cases of ST 11.1 + A 11.2 and ST 12.1 + A 12.2 treatment is a large increase in strength properties (σ_{UTS} and $\sigma_{0.2\%}$) corresponding to a large decrease in ductility property (ε_f) compared to the ST 11.1 and 12.1 treatment cases. Although the degradation of secondary α''-Ti phase and back to the initial α-

Ti phase (see Fig. 8.4.c and 8.4.f), but this increase/decrease in strength/ductility may be due to very fine precipitates in nanometre-sized generated from the α-Ti/ω-Ti phase in the β-Ti phase, as these precipitates represent material strengthening particles (the mechanism of age hardening).

8.2.2. Fracture surfaces analysis of thermomechanical processed cases

By examining the fracture surfaces obtained after tensile testing, one can assess the influence of thermomechanical processing route application on fracture behaviour in the tested samples.

8.2.2.1. Fracture surfaces analysis of as-received (AR) and hot deformation (HD3) cases

Fig. 8.5 shows specific images, at different magnifications, of the fracture surfaces obtained in the case of the as-received (AR) sample (Fig. 8.5.a and b) and the case of the hot-deformed (HD3) sample at 1000°C (Fig. 8.5.c and d).

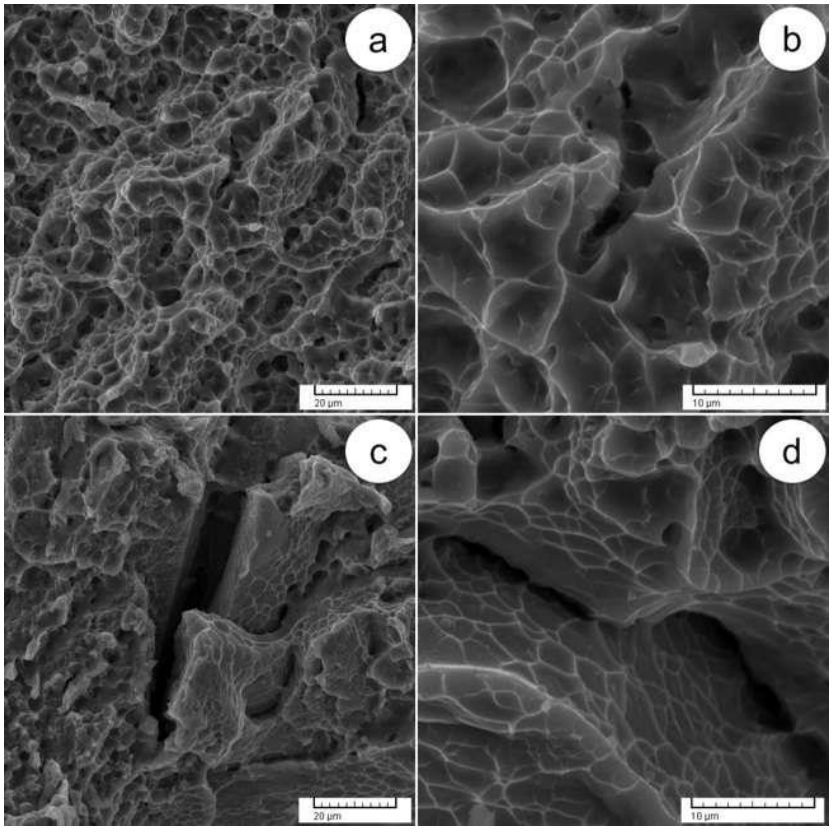

Fig. 8.5 *SEM-SE images of fracture surfaces after tensile testing of Ti-6246 alloy in AR case in different magnifications (a and b); HD3 case in different magnifications (c and d).*

In the case of AR, one can observe that the fracture surfaces analysis shows a fibrous morphology with a higher density of voids and dimples (Fig. 8.5.a), indicating a pronounced ductility. The mechanism of voids coalescence is observed (Fig. 8.5.b). Overall, the AR sample case shows ductile behaviour, confirming observations made during mechanical properties analysis (high strength of 1057±14MPa and high elongation to fracture of 12.9±1.8%). The case of the hot-deformed (HD3) sample at 1000°C shows, besides the fibrous areas, the presence of large crevices/fissures and cleavage areas/surfaces. Within the fibrous areas, one can observe small voids and shallow dimples, with a low density compared to the AR case (Fig. 8.5.c), also, voids coalescence areas (Fig. 8.5.d) indicating boundaries of prior deformed α-Ti/β-Ti colonies. Overall, the case of the HD3 sample shows a mixture of brittle-ductile

behaviour, confirming observations made during mechanical properties analysis (moderate strength of 1012±11MPa and low elongation to fracture of 3.2±0.6%).

8.2.2.2. Fracture surfaces analysis of solution treatment (ST) cases

Fig. 8.6 shows typical SEM-SE images of solution-treated (ST) fracture surfaces of Ti-6246 alloy at different temperatures and durations. Analysing the case of ST 7.1 treatment (see Fig. 8.6.a) performed at 800°C with treatment duration of 3min/1mm sample thickness, one can observe that the fracture surfaces show the presence of a large cleavage surface, large crevices/fissures and small fibrous areas. The fibrous areas show the presence of shallow dimples and small-size voids, and the presence of voids coalescence areas is also observed, indicating limited ductility. Analysing the size of all morphological aspects (cleavage surfaces, crevices/fissures and fibrous surfaces), one can conclude that the ST 7.1 treatment case shows a mixture of brittle-ductile behaviour. In the case of ST 9.1 treatment (see Fig. 8.6.b) performed at 900°C with treatment duration of 3mins/1mm sample thickness, one can observe that the fracture surfaces show similar morphological aspects with the case of ST 7.1 treatment, but with larger-size cleavage surfaces and lower-size fibrous areas. The fibrous areas show the presence of small-size voids and shallow dimples in comparison with ST 7.1 case, confirming the low/limited ductility (elongation to fracture) obtained in this case in comparison with ST 7.1 case. Case of ST 11.1 treatment (see Fig. 8.6.c), performed at 1000°C with treatment duration of 3mins/1mm sample thickness, shows that the morphological aspects observed on the fracture surfaces are mostly cleavage surfaces, and the fibrous areas being at a minimum. In-depth analysis of fibrous areas still shows the presence of small-size voids and shallow dimples. Overall, the case of S T11.1 treatment shows a pronounced brittle behaviour and low/limited ductility, confirming the observations made in mechanical properties analysis (moderate strength of 961±12MPa and low elongation to fracture of 7.2±0.9%).

Observations of the case of ST 8.1 treatment (see Fig. 8.6.d) performed at 800°C with treatment duration of 6mins/1mm sample thickness indicate that fracture surfaces contain a large cleavage surface and large/small-sized crevices/fissures along with small fibrous areas contain small-sized voids and shallow dimples in addition to the presence of the voids coalescence mechanism and based on the morphological examination, one can find that the case of ST 8.1 treatment exhibits limited ductility and the mixed character of brittle-ductile behaviour. The fracture surface analysis of the ST 10.1 treatment case (see Fig. 8.6.e) performed at 900°C with treatment duration of 6mins/1mm sample thickness presents some morphological aspects similar to the ST 8.1 treatment, where the cleavage surfaces are small in size and the fibrous areas are higher in density. Within the fibrous areas, voids of various sizes and shallow dimples of small size are also found. It can notice that this case has limited ductility versus ST 8.1 case. By examining the SEM-SE images of the ST 12.1 treatment case (see Fig. 8.6.f) performed at 1000°C with treatment duration of 6mins/1mm of sample thickness, one can see that the morphological observations of fracture surface mostly involve cleavage surfaces. Considering the fibrous areas, they still contained shallow dimples and small-sized voids but with much lower density compared to the ST 8.1 and ST 10.1 treatment cases. The case of ST 12.1 treatment presents a cleared brittle behaviour and a low/limited ductility, supporting observations made in mechanical properties analysis (moderate strength of 998±11MPa and low elongation to fracture of 7.8±1.1%).

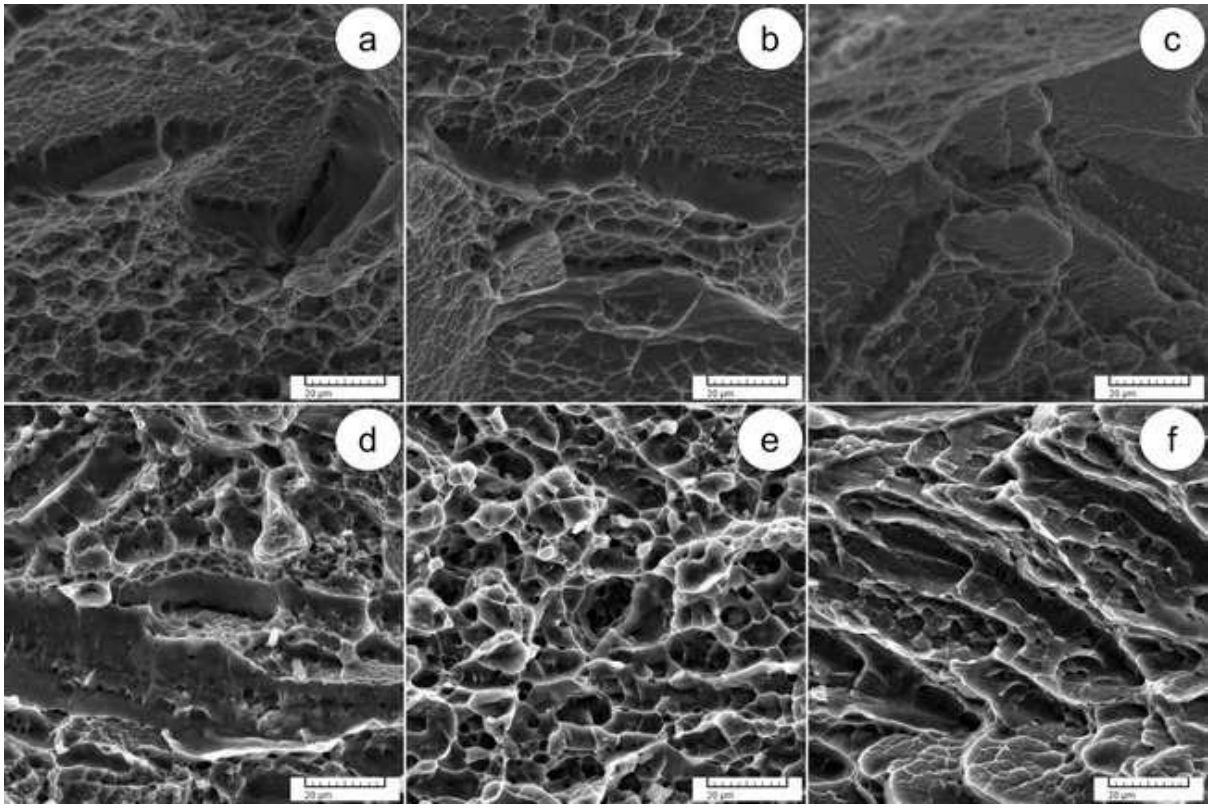

Fig. 8.6 *SEM-SE images of fracture surfaces after tensile testing of Ti-6246 alloy in (ST 7.1) case (a); (ST 9.1) case (b); (ST 11.1) case (c); (ST 8.1) case (d); (ST 10.1) case (e); (ST 12.1) case (f).*

8.2.2.3. Fracture surfaces analysis of ageing (A) cases

Fig. 8.7 shows typical SEM-SE images of ageing-treated (A) fracture surfaces of Ti-6246 alloy at constant temperature and duration after solution treatment (ST). Analysis of SEM-SE images of the ageing treatment case (ST 7.1 + A 7.2 - see Fig. 8.7.a) demonstrates the appearance of small-sized cleavage surfaces with high density, as well as voids are of higher density and small-sized and dimples are shallow within fibrous areas compared to the case of solution treatment (ST 7.1), with the observation of the voids coalescence areas. This case possesses mixed behaviour of the brittle-ductile type. The ageing treatment case (ST 9.1 + A 9.2 – see Fig. 8.7.b) shows large cleavage surfaces and fibrous areas. The fibrous areas morphology shows the presence of small-sized dense voids, small dimples and voids coalescence, indicating an increase in ductility compared to the case of solution treatment (ST 9.1). In the case of ageing treatment (ST 11.1 + A 11.2 – see Fig. 8.7.c), one can see a higher density of large and small-sized cleavage surfaces and larger areas of the voids coalescence phenomenon, besides the limited increase of voids and dimples, recording a decrease in ductility comparing with the case of solution treatment (ST 11.1) as the cleavage surfaces of small size may be the result of α-Ti/ω-Ti phase precipitation in the β-Ti phase, increasing the brittle behaviour of Ti-6246 alloy.

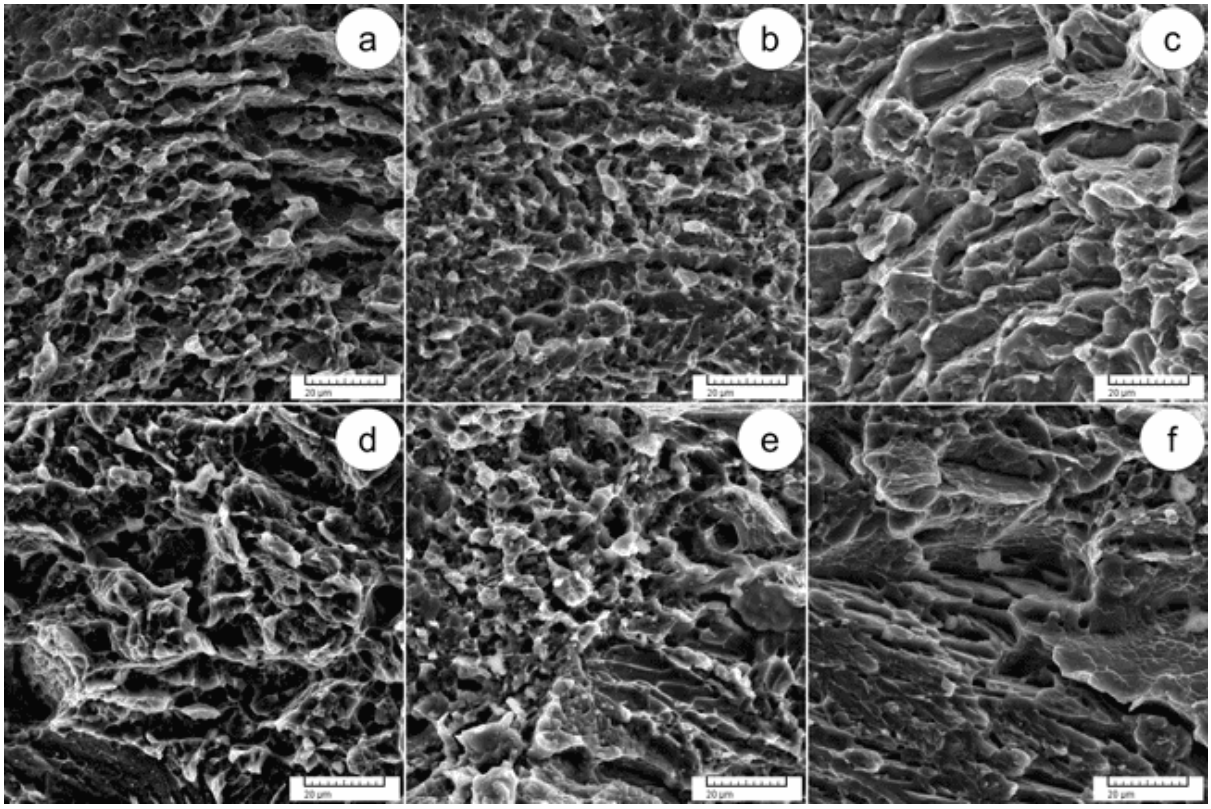

Fig. 8.7 *SEM-SE images of fracture surfaces after tensile testing of Ti-6246 alloy in (A 7.2) case (a); (A 9.2) case (b); (A 11.2) case (c); (A 8.2) case (d); (A 10.2) case (e); (A 12.2) case (f).*

Observations regarding the case of ST 8.1 + A 8.2 ageing treatment (see Fig. 8.7.d) are the presence of small-sized cleavage surfaces with high density. In addition to the cleavage surfaces, in this case, small-sized dimples and voids of high density and small-sized are also found within the fibrous areas, appearing a limited increase in ductility compared to the case of ST 8.1 solution treatment. The mechanical nature of this case is of the brittle-ductile type. Analysing the fracture surface for the case of ST 10.1 + A 10.2 ageing treatment (see Fig. 8.7.e), one can see large cleavage surfaces, dense fibrous areas and voids coalescence mechanism. Within the fibrous areas, voids and dimples of small sizes can see, indicating an increase in ductility comparing with the ST 10.1 solution treatment case. Considering the case of ST 12.1 + A 12.2 ageing treatment (see Fig. 8.7.f), one can see that the fracture surface mostly contains cleavage facets. It can also see that the fibrous areas in minimal and contain low-density voids, shallow dimples and larger aspects of the voids coalescence mechanism, resulting in a decrease in ductility compared to the case of ST 12.1 solution treatment. The α-Ti/ω-Ti phase precipitation in the β-Ti phase may have a role in forming small-sized cleavage facets, resulting in brittle behaviour.

8.3. Conclusions

The consequences of hot deformation above the β-transus temperature at 1000°C followed by solution and ageing treatments on the microstructural and mechanical properties evolution of Ti-6246 alloy are investigated in order to assess the effects that result from the application of the present thermomechanical processing route, and the summarised conclusions are as follows:

- Solution treatment (ST) cases, performed at temperatures below the Ti-6246 alloy transition temperature (at 800°C), increase the ductility property, and the α'-Ti phase is generated besides the main α-Ti and β-Ti phases, contributing to a relatively large increase in strength properties compared to the case of hot deformation of Ti-6246 alloy. It is also concluded that the α'-Ti phase is generated besides the main α-Ti and β-Ti phases in the solution treatment (ST) cases, performed close to the Ti-6246 alloy transition temperature (at 900°C) and have presented the highest strength and ductility properties between solution treatment cases.
- When the solution treatment is performed at temperatures above the Ti-6246 alloy transition temperature (at 1000°C), the α''-Ti phase generated besides the main α-Ti and β-Ti phases leads to a decrease in strength properties compared to the hot deformation case and solution treatment cases, performed below the alloy transition temperature, and these cases also present limited ductility.
- The cases of solution treatment performed at temperatures of 800°C, 900°C and 1000°C with treatment duration of 18mins and rapid cooling showed an increase in the strength and ductility properties compared to the cases of solution treatment performed under the same conditions but with treatment duration of 9mins.
- When the ageing treatment is performed at 600°C for 6h and air quenching, α'-Ti/α''-Ti $\rightarrow$ α-Ti/β-Ti and β-Ti $\rightarrow$ α-Ti/ω-Ti phasic transformations take place along with behaviours of stress-relieving and age-hardening, leading to various consequences for the evolution of the mechanical properties of Ti-6246 alloy serving to balance the mechanical properties.
- In ageing treatment, strength and ductility properties may be slightly increased or decreased because ageing treatment endeavours to provide a better combination of mechanical properties.

Chapter 9: General conclusions, personal contributions, recommendations and future research directions

9.1. General conclusions

The thesis deals centrally with the investigation of how thermomechanical processing parameters affect the alloy's microstructure, thus showing the mechanical properties of Ti-6246 alloy. As a key influence parameter in the route of thermomechanical processing, the thesis considers β-transus temperature, being a key parameter in both mechanical processing by hot-deformation and thermal processing by treatments of annealing, solution and ageing.
The following key general conclusions are emerging from the thesis:

- The mechanical processing by hot plastic deformation at temperatures between 800°C - 1100°C (from well below to well above the β-transus temperature ≈ 935°C), such as: 800°C (well below β-transus ≈ 935°C), 900°C (below close to β-transus ≈ 935°C), 1000°C (above β-transus ≈ 935°C) and 1100°C (well above β-transus ≈ 935°C). In the hot deformation performed below the β-transus temperature (at 800°C and 900°C), low-intensity deformations occurred in initial grains and α-Ti/β-Ti microstructural colonies when compared with the deformation intensity observed in the hot deformation

performed above the β-transus temperature (at 1000°C and 1100°C). *Therefore, one can assume that when envisioning high-intensity deformation, the chosen deformation temperature must be above β-transus temperature*.

- Increasing the hot deformation temperature from 800°C to 1100°C leads to a decrease in alloy's strength properties (ultimate tensile strength, yield strength and microhardness) and an increase in the alloy's ductility properties (elongation to fracture) due to the induced change in the alloy's constituent α-Ti and β-Ti phases fraction, increasing the temperature above the β-transus increases the β-Ti phase fraction. The observed behaviour in the exhibited mechanical properties is owned by the crystallography of the alloy's constituent phases, where α-Ti phase belongs to the HCP system, while β-Ti phase to the BCC system, which exhibits a higher intrinsic plasticity/ductility but a lower strength.
- Applying a thermal treatment by annealing treatment (AT) at a temperature above close to the β-transus temperature, after hot deformation, influences the α-Ti and β-Ti phases fractions in the Ti-6246 alloy, resulting in a consolidation of the α-Ti/β-Ti constituent colonies, and also decreases the internal defects density with a significant effect on the exhibited mechanical properties. No precipitations were observed for secondary phases. When comparing the results obtained with ones obtained before the annealing treatment, one can observe that all mechanical properties generally increase. The highest observed increase in strength properties was in the case of hot deformation at 1100°C (HD4) followed by annealing treatment (AT4) (i.e. ultimate tensile strength from 1001±11MPa to 1221±11MPa), while the highest observed increase in the ductility property was in the case of hot deformation at 800°C (HD1) followed by annealing treatment (AT1) (i.e. elongation to fracture from 3.5±0.8% to 8.3±1.1). *Overall, one can assume that by applying annealing treatment at a temperature close to β-transus, one can stir the mechanical behaviour towards an appropriate combination of mechanical properties*.
- When applying a thermal treatment by solution treatment (ST) at temperatures well below (800°C), below close to (900°C) and above (1000°C) β-transus temperature on hot-deformed samples at 900°C (HD2), α-Ti/β-Ti constituent colonies are consolidated due to solution treatment temperature and also α'-Ti and α''-Ti phases transformations occur, due to rapid cooling to ambient temperature. It has been shown that when the treatment duration is increased from 3min/1mm to 6min/1mm of samples thickness, this leads to a noticeable increase in strength properties but a negligible increase in ductility properties (i.e. ST1.1 compared to ST2.1: ultimate tensile strength 1165±13MPa to 1221±12MPa, elongation to fracture 5.3±1.1% to 5.8±0.9%). Also, the obtained highest strength properties were observed in the solution treatment (ST) performed close to β-transus temperature (i.e. ST3.1 - 1357±14MPa and ST4.1 - 1395±11MPa), while the obtained highest ductility properties were observed in the solution treatment (ST) performed above β-transus temperature (i.e. ST5.1 - 9.7±1.2% and ST6.1 - 10.4±1.4%). *Overall, one can assume that when envisioning strength properties, the solution treatment temperature chosen must be close to β-transus temperature, while when envisioning ductility properties, the solution treatment temperature chosen must be above β-transus temperature*.

- When applying a final thermal treatment by ageing treatment (A) at a temperature well below β-transus at 600°C to the solution-treated samples (ST), the α-Ti/β-Ti constituent colonies are consolidated due to ageing treatment temperature and also return the secondary α'-Ti and α''-Ti phases to the parent α-Ti/β-Ti phases due to ageing treatment temperature and duration, stress-relieving and age-hardening. In the case of ageing treatment performed on solution treated samples at temperatures below and close to β-transus (ST1.1, ST2.1, ST3.1 and ST4.1), it has been shown that strength properties are decreasing (i.e. ST1.1 - 1165±13MPa to A1.2 - 1089±11MPa) and ductility properties are increasing (i.e. ST1.1 - 5.3±1.1% to A1.2 - 8.1±1.3%). In the case of ageing treatment performed on solution treated samples at temperatures above β-transus (ST5.1 and ST6.1), it has been shown that strength properties are increasing (i.e. ST5.1 - 984±13MPa to A5.2 - 1170±11MPa) and ductility properties are decreasing (i.e. ST5.1 - 9.7±1.2% to A5.2 - 6.9±1.2%). *Overall, one can assume that by applying an ageing treatment at a temperature below β-transus, one can stir the mechanical behaviour towards an appropriate combination of mechanical properties.*
- When applying a thermal treatment by solution treatment (ST) at temperatures below (800°C), below close to (900°C) and above (1000°C) the β-transus temperature on the hot deformation samples at 1000°C (HD3), similar results were concluded in terms of microstructural aspect and slightly lower mechanical properties when compared with the ones obtained in the case of hot deformation at 900°C (HD2) and solution treated (ST) samples. One can observe that both strength and ductility are slightly lower (i.e. ultimate tensile strength: ST11.1 - 961±12MPa compared to ST5.1 - 984±13MPa; elongation to fracture: ST11.1 – 7.2±0.9% compared to ST5.1 – 9.7±1.2%). *Therefore, one can assume that when envisioning high-strength and/or high-ductility properties, the chosen deformation temperature must be below β-transus temperature*.
- During applying a final thermal treatment by ageing treating (A) at a temperature well below the β-transus temperature at 600°C on the solution-treated samples (ST) and the hot-deformed samples at 1000°C (HD3), similar results were also concluded in terms of microstructural aspect and slightly lower mechanical properties when compared with the ones obtained in the case of hot deformation samples at 900°C (HD2) and solution-treated (ST) samples. *Therefore, one can assume that when envisioning high-strength and/or high-ductility properties, the chosen deformation temperature must be below β-transus temperature*.
- Based on the obtained results in terms of microstructural and mechanical data, one can properly design a thermomechanical processing route consisting of hot-deformation followed by primary annealing and/or solution treatment and secondary ageing treatment in order to obtain a suitable combination of mechanical properties (i.e. both high-strength and high-ductility).

9.2. Personal contributions

A series of original/personal contributions, in terms of novelty, resulting from this thesis can be presented as follows:

- Conducting a complex literature study, focused on titanium-based alloys, mainly on Ti-6246 alloy, which belongs to the (α + β) class of titanium alloys, in order to determine the most influential thermomechanical processing parameters when designing a route that combines mechanical and thermal processing applied to Ti-6246 alloy, aiming to obtain a suitable combination of mechanical properties.
- Development of original experimental programs considering existing laboratory infrastructure in order to achieve the assumed objectives.
- Investigation of the effects induced by hot deformation in the case of Ti-6246 alloy in an experimental space ranging from a temperature well below the β-transus (800°C) to well above the β-transus (1100°C).
- Investigation of the effects induced by the solution treatment on microstructure and exhibited mechanical properties, in a wide range of treatment temperatures ranging from 800°C to 1000°C, with different treatment durations of 3mins/mm and 6mins/mm.
- Investigation of the effects induced by a secondary ageing treatment applied after primary solution treatment on microstructure and exhibited mechanical properties.
- Obtaining proper thermomechanical processed samples of Ti-6246 alloy to be used in assessing the effects induced by thermomechanical processing based on the developed experimental programs.
- Developing the specific investigation and characterisation procedures applied to thermomechanically processed Ti-6246 alloy samples in order to obtain data about microstructure and mechanical properties focused on OM, SEM, XRD, tensile and microhardness testing.

9.3. Recommendations

The performed experiments in the case of Ti-6246 alloy have shown that it is possible to obtain a suitable combination of mechanical properties (i.e. high-strength and high-ductility) when a well-chosen thermomechanical processing route is applied. The following general recommendations can present:

- When the intention is only to deform the Ti-6246 alloy, the hot deformation processing must be conducted/performed at a temperature above the β-transus, due to the crystallography of the α-Ti/β-Ti alloy's constituent phases, α-Ti phase belongs to the HCP system, while β-Ti phase to the BCC system, which exhibits a higher intrinsic plasticity/ductility.
- When the intention is to deform the Ti-6246 alloy, but also to obtain high strength properties, then hot deformation processing must be conducted/performed in two stages: 1) the first stage at a temperature above β-transus to achieve high deformation intensity; 2) the second stage at a temperature below or close to β-transus to achieve the desired final shape, after hot deformation, it is followed by the application of primary heat treatment consisting of treatment of annealing or solution, performed at a temperature close to a β-transus temperature, which will be increasing the strength and ductility properties. If higher ductility is needed, then ageing treatment must be performed as a secondary treatment, which will be further increasing ductility properties but will slightly decrease strength properties.

9.4. Future research directions

The future directions to continue researches in the field of thermomechanical processing and characterisation of Ti-6246 alloy can be summarised as follows:

- In addition to conventional examination methods, such as optical microscopy (OM), scanning electron microscopy (SEM), X-ray diffraction (XRD), one can involve other advanced investigation techniques, such as: transmission electron microscopy (TEM), electron backscatter diffraction (EBSD), and other descriptive-analytical methods in order to accurately study the alloy's microstructural constituents (phase morphology, crystallography, etc.), secondary phase precipitation, the occurrence of deformation mechanisms (slipping/twinning), dislocation propagation, etc., about giving further insight into understanding the relation of mechanical properties to microstructure.
- In a similar series of investigations performed within the experimental programs, one may extend the study of increasing the duration of annealing/solution treatment on the microstructure evolution and the exhibited mechanical properties of Ti-6246 alloy. Also, one may consider the influence of cooling conditions, considering that the dynamic and static recrystallisation take place under these assumed conditions, which will be introducing a new level of complexity to the analysis procedure.
- It is possible to expand the research by modifying the mechanical processing and thermal processing steps of Ti-6246 alloy with additional processing steps, which may give a better combination of properties, thus expanding the possible end-user applications.
- It is possible to expand the research by modifying the chemical composition of Ti-6246 alloy with additional alloying elements/contents, which may give better insight into various possible end-user applications.

Selected References

Ahmed, Y. M., Sahari, K. S. M., Ishak, M., Khidhir, B. A. Titanium and its Alloy, International Journal of Science and Research (IJSR), Vol. 3, Iss. 10, 2012, pp. 1351-1361.

Askeland, D. R., Fulay, P. P., Wright, W. J. The Science and Engineering of Materials, Cengage Learning, Inc., USA, 2010, p. 949.

Bein, S., Béchet, J. Phase transformation kinetics and mechanisms in titanium alloys Ti-6.2.4.6, β-CEZ and Ti-10.2.3., Journal de Physique IV Colloque, J. Phys. IV France, Vol. 06, No. C1, 1996, pp. C1-99 - C1-108.

Boyer, R., Collings, E. W., Welsch, G., Lampman, S. Materials properties handbook: Titanium alloys, 1st Ed., ASM International, Materials Park, OH, USA, 1994, p 788.

Cherukuri, B. Microstructural stability and thermomechanical processing of boron modified beta titanium alloys, (Ph.D. thesis), Department of Mechanical and Materials Engineering, Wright State University, USA, 2008.

Donachie, M. J. Titanium: A technical guide, 2nd Ed., ASM International, Materials Park, OH, USA, 2000, p. 216.

Ezugwu, E. O., Wang, Z. M. Titanium alloys and their machinability - A review, Journal of Materials Processing Technology, Vol. 68, Iss. 3, 1997, pp. 262-274.

Flower, H. M. Microstructural development in relation to hot working of titanium alloys, Materials Science and Technology, Vol. 6, No. 11, 1990, pp. 1082-1092.

Groover, M. P. Fundamentals of Modern Manufacturing: Materials, Processes, and Systems, 4th Ed., John Wiley & Sons, Inc., USA, 2007, p. 1025.

Guuo, Y. Microstructure characterisation of linear friction welded titanium alloys using EBSD and TEM, (Ph.D. thesis), University of Birmingham, Birmingham, UK, 2012.

Ishida, T., Wakai, E., Makimura, S., Casella, A. M., Edwards, D. J., Prabhakaran, R., Senor, D. J., Ammigan, K., Bidhar, S., Hurh, P. G., Pellemoine, F., Densham, C. J., Fitton, M. D., Bennett, J. M., Kim, D., Simos, N., Hagiwara, M., Kawamura, N., Meigo, S., Yonehara, K. Tensile behavior of dual-phase titanium alloys under high-intensity proton beam exposure: Radiation-induced omega phase transformation in Ti-6Al-4V, Journal of Nuclear Materials, Vol. 541, 2020, p. 152413.

Jackson, M., Dashwood, R. J., Christodoulou, L., Flower, H. M. Thermomechanical processing of titanium alloys: the Application of a novel technique to examine sub-β transus isothermal forging of Ti-6AI-2Sn-4Zr-6Mo, in: Titanium Alloys at Elevated Temperature: Structural Development and Service Behaviour, editor by M. R. Winston, and A. Strang, 1st Ed., Institute of Materials (IOM) Communications Ltd, UK, London, 2001, pp. 89-101.

Joshi, V. A. Titanium alloys: an atlas of structures and fracture features, CRC Press -Taylor & Francis Group, 6000 Broken Sound Parkway NW, Suite 300 Boca Raton, FL 33487-2742, 2006.

Leyens, C., Peters, M. Titanium and titanium alloys - Fundamentals and Applications, WILEY-VCH Verlag GmbH & Co. KGaA, Weinheim, Germany, 2003.

Liu, A. F. Mechanics and Mechanisms of Fracture: An Introduction, 1st Ed., ASM International, Materials Park, OH, USA, 2005.

Lütjering, G., Williams, J. C. Titanium, Springer-Verlag Berlin Heidelberg, Germany, 2007, p. 449.

Mullen, M. J., Griebel, A. H., Tartaglia, J. M. Fracture surface analysis, Advanced Materials and Processes (ASM International), Stork Climax Research Services, Wixom, Michigan, Vol. 165, Iss. 11, 2007, pp. 21-23.

Pardhi, Y. U. Microstructure evolution and its effect on fatigue performance in inertia welds of Titanium and Nickel based alloys, (Ph.D. thesis), University of Birmingham, Birmingham, UK, 2010.

Partridge, P. G. The crystallography and deformation modes of hexagonal close-packed metals, Metallurgical Reviews, Vol. 12, No. 1, 1967, pp. 169-194.

Pederson, R. The microstructures of Ti-6A1-4V and Ti-6Al-2Sn-4Zr-6Mo and their relationship to processing and properties, (Ph.D. thesis), Department of Applied Physics and Mechanical Engineering, Division of Engineering Materials, Luleå University of Technology, Sweden, 2004.

Peters, M., Hemptenmacher, J., Kumpfert, J., Leyens, C. Structure and properties of titanium and titanium alloys, in: Titanium and Titanium Alloys, 1st Ed., Editor by Leyens, C., and Peters, M., Wiley-VCH Verlag GmbH & Co. KGaA, Weinheim, Germany, 2003, pp. 1-36.

Richardson, M. D. Microstructural and Mechanical Property Development in Metastable Beta Titanium Alloys, (Ph.D. thesis), Department of Materials Science and Engineering, University of Sheffield, UK, 2016.

Roder, O., Helm, D., Lütjering, G. Titanium '03: Science and Technology, Proceedings of the 10th World Conference on Titanium, Held at the CCH-Congress Center, Hamburg, Germany July, Proceeding currently in press, Wiley VCH, Vol. 1, 2003, pp. 13-18.

Semiatin, S. L., Seetharaman, V., Weiss, I. The thermomechanical processing of alpha/beta titanium alloys, Journal of The Minerals, Metals & Materials (JOM), Vol. 49, Iss. 6, 1997, pp. 33-39.

Veiga, C., Davim, J. P., Loureiro, A. G. R. Properties and applications of titanium alloys: A brief review, Reviews on advanced materials science, Vol. 32, No. 2, 2012, pp. 133-148.

Walter, J. L., Jackson, M. R., Sims, C. T. Titanium and its Alloys: Principles of Alloying Titanium, 1st Ed., ASM International, Metals Park, Ohio, USA, 1988.

Weiss, I., Semiatin, S. L. Thermomechanical processing of alpha titanium alloys - an overview, Materials Science and Engineering: A, Vol. 263, Iss. 2, 1999, pp. 243-256.

Weiss, I., Semiatin, S. L. Thermomechanical processing of beta titanium alloys - an overview, Materials Science and Engineering: A, Vol. 243, Issues 1-2, 1998, pp. 46-65.

Welsch, G., Boyer, R., Collins, E. W. Materials Properties Handbook: Titanium Alloys, ASM International, Materials Park, OH, USA, 1994.

Results dissemination

A) Published scientific papers within high impact factor (IF) journal:

1. **Mohammed Hayder ALLUAIBI**, Elisabeta Mirela COJOCARU, Adrian RUSEA, Nicolae Șerban, George Coman and Vasile Dănuț COJOCARU. *Microstructure and Mechanical Properties Evolution during Solution and Ageing Treatment for a Hot Deformed, above β-transus, Ti-6246 Alloy*, ***Metals***, 2020, Vol. 10, No. 9, p. 1114.

B) Published scientific papers within ISI journal:

1. **Mohammed Hayder ALLUAIBI**, Adrian RUSEA, Vasile Danut COJOCARU. *Influence of thermomechanical processing at temperatures above β-transus on the microstructural and mechanical characteristics of the Ti-6246 alloy*, ***University Politehnica of Bucharest Scientific Bulletin Series B - Chemistry and Materials Science***, 2018, Vol. 80, No. 1, pp. 245-258.
2. **Mohammed Hayder ALLUAIBI**, Saleh Sabah ALTURAIHI, Elisabeta Mirela COJOCARU and Ion CINCA. *Microstructural evolution during thermomechanical processing of Ti-6246 titanium alloy*, ***University Politehnica of Bucharest Scientific Bulletin: Series B - Chemistry and Materials Science***, 2019, Vol. 81, No. 1, pp. 225-234.
3. Saleh Sabah ALTURAIHI, **Mohammed Hayder ALLUAIBI**, Elisabeta Mirela COJOCARU and Doina RADUCANU. *Microstructural changes occurred during hot-deformation of SDSS F55 (super-duplex stainless steel) alloy*, ***University Politehnica of Bucharest Scientific Bulletin Series B - Chemistry and Materials Science***, 2019, Vol. 81, No. 1, pp. 149-160.
4. **Mohammed Hayder ALLUAIBI**, Saleh Sabah ALTURAIHI, Adrian RUSEA, Elisabeta Mirela COJOCARU. *The response of microstructure and mechanical properties of Ti-6246 alloy to thermomechanical processing*, ***University Politehnica of Bucharest Scientific Bulletin: Series B - Chemistry and Materials Science***, 2021, Vol. 83, No. 2, pp. 231-242.

C) Published scientific papers in international conferences within the index of Scopus and Clarivate:

1. **Mohammed Hayder ALLUAIBI** and Vasile Dănuț COJOCARU. *Effect of thermomechanical processing and heat treatment on the microstructure evolution of the Ti-6246 alloy*, ***IOP Conference Series: Materials Science and Engineering, Istanbul***, Turkey, Vol. 454, 2018.
2. **Mohammed Hayder ALLUAIBI**, Saleh Sabah ALTURAIHI, Doina RADUCANU, Adrian RUSEA, Ion CINCA, Anna NOCIVIN, Vasile Danut COJOCARU. *Microstructure investigation and mechanical properties of Ti-6Al-2Sn-4Zr-6Mo alloy processed by hot rolling and solution treatment*, ***Metal***, Brno, Czech Republic, 2020.